Russian Chemical Reviews **78** (9) 833 – 854 (2009) © 2009 Russian Academy of Sciences and Turpion Ltd

DOI 10.1070/RC2009v078n09ABEH004077

Preparation and properties of single-walled nanotubes filled with inorganic compounds

A A Eliseev, M V Kharlamova, M V Chernysheva, A V Lukashin, Yu D Tretyakov, A S Kumskov, N A Kiselev

Contents

I.	Introduction	833
II.	Filling single-walled carbon nanotubes during their growth (*in situ*)	835
III.	Filling pre-synthesized single-walled nanotubes (*ex situ* methods)	836
IV.	Structures and properties of '1D-crystal@SWNT' nanocomposites	843
V.	Investigations into functional properties of '1D-crystal@SWNT' composites	847
VI.	Conclusion	851

Abstract. The state-of-the-art methods for filling single-walled carbon nanotubes (SWNTs) are analyzed systematically. *In situ* and *ex situ* approaches for filling SWNTs are addressed. They are based on both intercalation of inorganic substances from the gas phase, solution or melts inside SWNTs and the formation of nanocrystals inside the channels as a result of chemical reactions. A comparative evaluation of these methods is performed, and major requirements for successful formation of '1D-crystal@SWNT' nanocomposites are formulated. The functional properties of the intercalated single-walled nanotubes and their possible applications in modern nanotechnologies are discussed. The bibliography includes 150 references.

I. Introduction

Single-walled carbon nanotubes (SWNTs) obtained for the first time in 1993 by graphite arc-discharge evaporation in the presence of a catalyst [1, 2] are currently among the most exciting and promising nanostructures. They generate huge interest of researchers all over the world due to their unique atomic structures (SWNTs feature maximum geometric anisotropy factors among the known nanostructures) and unusual chemical, electronic (thermal and electric conductivity), also mechanical properties (high values of Young's modulus, tensile and compressive strengths, high cracking resistance, *etc*.). The unique properties of carbon nanotubes (CNTs) are governed by not only their unusual tubular structures, but also by the virtually total absence of structural defects.[3 – 5] All this makes CNTs potentially useful as elements of nanoelectronics (logical gates, memory devices, emitters, nanowires), nanoelectromechanical systems, nanocomposite fillers (for strengthening and functionalizing bulk materials), probe tips for scanning probe microscopy, *etc*. SWNTs found one of the major technological applications in the development of a new generation of field-effect transitors.[6]

Single-walled carbon nanotubes constitute one-atom-thick graphite sheets (called graphene) wrapped into seamless cylinders that are from 0.4 to several nanometers in diameter and up to several tens and even hundreds of micrometers in length. The orientation of the hexagonal lattice of graphene relative to the longitudinal axis of a nanotube determines the nanotube chirality (the chiral vector of the graphene sheet).

The electronic properties of defectless SWNTs are extremely sensitive to their geometric structures and are determined by nanotube chiralities.[4, 7] Depending on their structure, carbon NTs can exhibit both metallic and semiconductor conductivities.[8 – 10] The dependence of the electronic properties of SWNTs on the chiral vector (particularly, on the diameter of a nanotube) can be regarded as both an advantage and a serious drawback of carbon nanotubes, since so far there are no efficient methods for the preparation and isolation of SWNTs bearing a desired chirality.[11, 12] In this connection, much attention is given to development of methods for separation of a whole array of SWNTs into semiconducting and metallic nanotubes and also for the methods of modification of electronic properties of SWNTs that would not require their separation by chirality.[13, 14]

Currently, there are two techniques for the separation of NTs, *viz*., burning off carbon NTs with a metallic conduc-

A A Eliseev, M V Kharlamova, M V Chernysheva, A V Lukashin, Yu D Tretyakov Department of Materials Science, M V Lomonosov Moscow State University, Leninskie Gory, 119991 Moscow, Russian Federation. Fax (7-495) 939 09 98, tel. (7-495) 939 52 48, e-mail: eliseev@inorg.chem.msu.ru (A A Eliseev), x-mari-mir@yandex.ru (M V Kharlamova), chernysheva@inorg.chem.msu.ru (M V Chernysheva), tel. (7-495) 939 59 31, e-mail: alex@inorg.chem.msu.ru (A V Lukashin), tel. (7-495) 939 20 74, e-mail: yudt@inorg.chem.msu.ru (Yu D Tretyakov)
A S Kumskov, N A Kiselev A V Shubnikov Institute of Crystallography, Russian Academy of Sciences, Leninsky prosp. 59, 119333 Moscow, Russian Federation. Fax (7-499) 135 10 11, tel. (7-495) 135 10 25 (A S Kumskov), (499)135 – 1520, e-mail: kiselev@ns.crys.ras.ru (N A Kiselev)

Received 14 May 2009
Uspekhi Khimii **78** (9) 901 – 923 (2009); translated by A F Nasonov

tivity by current-induced oxidation while retaining the semiconducting tubes and ultracentrifugation using surfactants, resulting in separation of NTs according to the conductivity type and nanotube diameters.[15]

Modification of nanotube structures forms the basis for directed changes in their electronic properties. Back in 1996, possible development of the electronic p–n-junction between SWNTs having different chiralities was considered;[16,17] such a transition has recently been implemented experimentally in a single SWNT.[12,18] Since the conductivity type is dependent on the chirality of a nanotube, one should change the nanotube structure on a certain segment in order to form the electronic p–n-junction. Such a change is possible due to creation of paired defects as five- or seven-membered rings in the graphene layer.[17,18] In this case, two segments of an NT will have different chiralities and different electronic structures, which will result in electronic transitions of the type 'metal–metal', 'metal–semiconductor' or 'semiconductor–semiconductor'. A carbon nanotube with 'metal–semiconductor' junction possesses the properties of a molecular diode.[19] In addition to the diode, more complex systems such as logic gates can also be developed.[18,20] To date, prototypes of diodes, transistors and simplest logical schemes based on carbon NTs have already been created.[21–25] However, the controlled incorporation of defects into an NT structure is an unattainable goal yet.

A simpler way of the controlled modifications of SWNT properties is filling the nanotubes with appropriate substances followed by their electron beam-induced local deintercalation.[26,27]

Intercalation of a substance into a nanotube can result in either a complete change in its band structure (for the effective interaction of the intercalated substance with the nanotube walls, as, for instance, in the case of fluorination of the tubes),[28] or only a shift of the electron density in the approximation of a rigid band structure,[29,30] which leads to the shift of the Fermi level of the tube.†

In the simplest case, intercalation of an electron donor with the Fermi level higher than that of an SWNT into metallic nanotubes leads to an increase in electron density on the tube walls, which results in an increase in the nanomcomposite conductivity, whereas incorporation of an electron acceptor with the Fermi level lower than that of an SWNT can bring about the nanocomposite transition into a semiconducting state.[13,32,33] Thus, this approach based on electron transfer upon the introduction of electron-donor or electron-acceptor compounds (metals, semiconductors, dielectrics) into single-walled nanotube channels enables control of the electronic structures of SWNTs and appearance, in the case of partial filling of the channels (for example, if a nanotube is half-filled), of p–n-junctions inside a single nanotube.

The chemical design of SWNTs by filling them with appropriate electroconductive, optical or magnetic materials enables the development of a new class of functionalazed on nanotubes, which have prospects as active elements of electronic devices and circuits. The small internal diameters (starting from 0.4 nm) of nanotubes make them exceptionally attractive as templates in the formation of one-dimensional nanocrystals incorporated in nanotubes — 'one-dimensional crystal@SWNTs' (from this point on, '1D-crystal@SWNTs').[34] The formation of nanocrystals inside nanotubes results from slow crystallization of a substance drawn into NTs from the gas or liquid phases by capillary forces.[35]

On crystallization of compounds inside a nanotube, the reaction zone is restricted by the NT walls, which creates conditions similar to those for the synthesis in a one-dimensional nanoreactor.[14] Thus, it becomes possible to directly influence the structures of nanoparticles that crystallize and control their shapes and anisotropy.[34,36,37]

A section of a one-dimensional nanocrystal can be represented as a polyhedron. Its incorporation into the internal cavity of an SWNT results in a local distortion of the graphene layer of the nanotube (the nanotube surface conforms to the nanocrystal shape).[38] Intercalation of a crystal having the section larger than the internal diameter of a nanotube will lead to certain stretching of the nanotube walls and the reduction of the crystal lattice parameter of the nanocrystal, and conversely, the intercalation of a crystal having the section somewhat smaller than the diameter of the channel will result in the compression of the nanotube (provided that the crystal effectively interacts with the graphene layer).

Taking into account that the mechanical properties of nanotubes (for instance, tensile strength and elastic modulus) depend on interatomic distances in the graphene layer, the mechanical properties of the produced nanocomposites can be varied by incorporating one or another crystalline inorganic compound into SWNTs.[20]

Synthesis of nanocomposites based on SWNTs by filling them with conductive, optical or magnetic materials opens up the way to creating a new class of nanostructures with properties not characteristic of unfilled SWNTs [for example, the intercalation of fullerides or magnetic nanoparticles (Fe, Co) into SWNT channels yields superconducting or ferromagnetic nanocomposites, respectively].[14,39–42] The incorporation of functional materials permits the control of the conductivity of the produced nanostructures with the aid of external impacts, for instance, a magnetic field or illumination.

The original article on the synthesis of filled nanotubes was published by Ajayan and Iijima in 1993,[43] who for the first time used multi-walled nanotubes as 'molecular containers' for lead. This experimental work confirmed the conclusions made on the basis of theoretical calculations[44] that sufficiently strong capillary forces exist in carbon nanotubes, which retain gases and liquids inside the channels. Later the idea of the controlled filling of carbon nanotubes with a wide variety of molecular compounds, nanoclusters or nanoparticles including fullerenes, metals (Pd, Pt, Ag, Au), metal oxides (ZrO_2, MoO_2, NiO, CdO, La_2O_3, Sm_2O_3) or metal halides (KI, AgCl, $ZrCl_4$, $CdCl_2$, $TbCl_3$) was developed by other researchers.[13,14,30,31,34,36,37,45,46]

Currently there are several methods for filling carbon nanotubes, which can be divided into two large groups:[14] filling nanotubes during their growth (*in situ* methods) and intercalation of compounds from the gas or liquid phases into cavities of pre-formed carbon nanotubes (*ex situ* methods).[47] Various methods for filling carbon nanotubes with inorganic compounds are presented in Fig. 1.

The present review is primarily focused on the nanocomposites based on single-walled nanotubes in which the

† A shift in the Fermi level in SWNTs filled with CrO_3, Ag or C_{60} was detected by the Raman spectroscopy.[14,30,31]

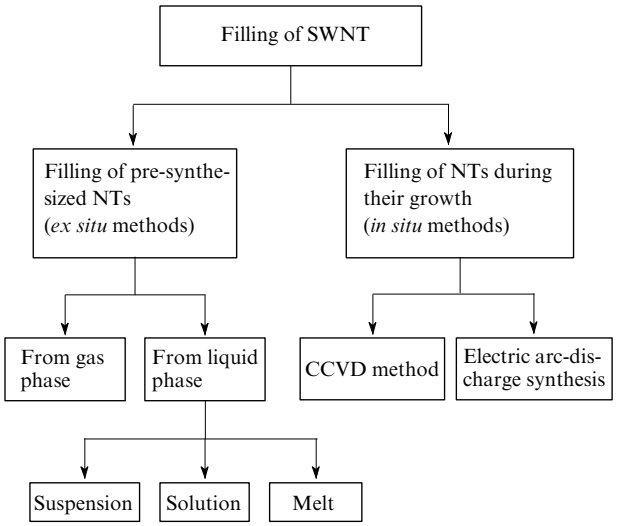


Figure 1. General scheme of the methods of carbon nanotube filling with various inorganic compounds.

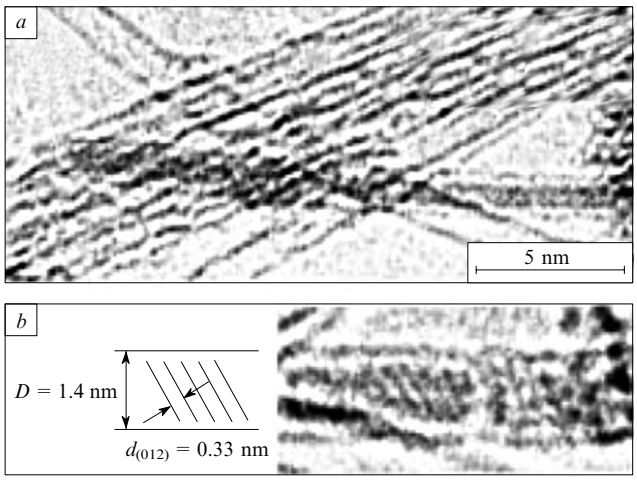


Figure 2. HRTEM images of SWNT bundles filled with bismuth by arc-discharge synthesis.[51]
The lattice spacing $d = 0.33$ nm corresponds to the interplanar spacing $d_{(012)}$ in the bulk bismuth crystal.

role of intercalated compounds can be seen more clearly (as compared to multi-walled nanotubes).

II. Filling single-walled carbon nanotubes during their growth (*in situ*)

Filling SWNTs during their catalytic growth (*in situ*) is the simplest of all the known approaches. To date, there are two methods for the fabrication of nanotubes that use the *in situ* strategy for the intercalation of inorganic compounds into nanotubes, *viz*., catalytic chemical vapour deposition (CCVD) of hydrocarbons and arc-discharge synthesis.[14]

It should be noted that the overwhelming majority of studies on filling nanotubes using the *in situ* methods deal with multi-walled nanotubes (MWNTs), whereas SWNTs are reported only in a few instances.[14] Normally, pyrolysis of a carbon source with simultaneous sublimation or decomposition of metal-containing compounds (for example, metal oxides, metal carbonyls or metallocenes) is employed for filling channels of multi-walled nanotubes by CCVD.[14, 48, 49] Most often, nanotubes filled with transition metals (Fe, Co, Ni) that are used as catalysts in the syntheses of SWNTs are obtained in this way;[49] however, examples of filling multi-walled nanotubes with Cu and Ge particles are known.[50] The use of CCVD for the preparation of '1D-crystal@SWNT' nanocomposites is limited due to the need of strict temperature control. The intercalation can occur only at the temperatures that are close to the melting points of intercalated compounds, while the sublimation (decomposition) temperatures of precursors must be close to those at which growth of SWNTs takes place. This altogether restricts the scope of carbon sources and compounds that can be intercalated.

Arc-discharge synthesis of carbon nanotubes filled with various compounds is carried out with graphite rods electrodes, the anode containing the compound to be intercalated (usually a metal) and a catalyst (Fig. 2).[51] It was this approach that allowed the preparation of single-walled carbon nanotubes for the first time.[1, 2] To date, a wealth of works on the application of arc-discharge synthesis to obtain filled multi-walled nanotubes has been published. Most often, in the arc-discharge synthesis the selected substance is incorporated into NTs as a carbide (Cr, Mn, Fe, Ni, Pd, Y, Gd, Dy, Yb, La, Ce). However, under certain conditions or by using compounds that do not tend to form carbides, the intercalation of elemental compounds (Se, Ge, Sb, Cr, Mn, Co, Cu, Re, Au, Sm, Gd, Dy, Yb) is also possible.[52, 53] The presence of catalytic amounts of sulfur in graphite anodes plays a key role in the formation of filled nanotubes (in the absence of sulfur, no filled MWNTs are obtained).[54] This is due to the necessity for wetting the surface of nanotube channels to allow the intercalation of the selected substance into the cavities of NTs, *i.e*., there is a need for a liquid phase (in this case, a metal–sulfur eutectic).‡ A disadvantage of this method is that it is impossible to control the filling process due to a large temperature gradient in the cathode area, which results in heterogeneous filling of nanotubes.[15] In addition, the arc-discharge technique does not enable the preparation of nanotubes filled with transition metals due to the formation of solid solutions metal–carbon and carbides with various compositions.[14] For their syntheses, CCVD is used. Thus, CCVD and arc-discharge synthesis are complementary in terms of the choice of starting compounds.[14, 54, 55] The *in situ* approaches do not allow formation of unstable species and complex chemical compounds (metal oxides, metal salts) inside nanotubes due to relatively high temperatures and reductive atmosphere maintained during nanotube syntheses, which is referred to as their disadvantage.

As has already been mentioned, only a few works are known that address the filling of single-walled nanotubes during their growth.[14, 46, 51] In these studies, the arc-discharge technique was used for generating composites 'one-dimensional crystal@SWNT'.[14] In 1999 SWNTs were filled with bismuth nanoparticles (see Fig. 2) possesing interplane distances of 0.33 nm (this value corresponds to the interplanar spacing $d_{(012)}$ in the three-dimensional crystal of bismuth),[51] in 2000 single-walled nanotubes filled with full-

‡ The majority of phase diagrams metal–sulfur have an eutectic the melting point of which is considerably lower than that of the pure metal.

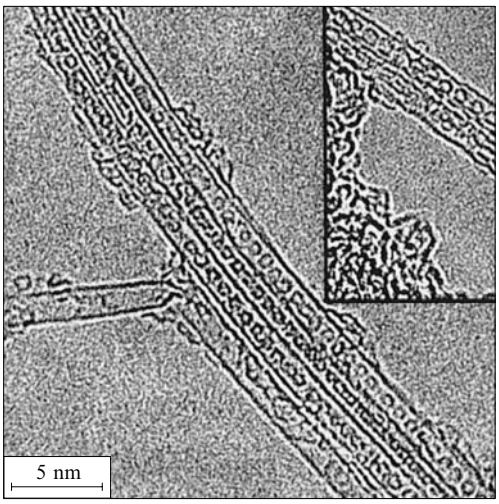


Figure 3. HRTEM micrographs of bundles of SWNTs filled with C_{60} fullerenes manufactured by arc-discharge technique.[46]

erenes C_{60} were obtained (the so-called 'nanopeapods') (Fig. 3).[46] It should be noted that the major drawback of the *in situ* strategy for filling single-walled nanotubes is its low efficiency: the yields of filled SWNTs are not more than several percent. These shortcomings of the *in situ* methods encouraged the development of *ex situ* approaches to filling SWNTs.

III. Filling pre-synthesized single-walled nanotubes (*ex situ* methods)

The most universal approach to obtaining filled nanotubes is the filling of pre-synthesized nanotubes (the *ex situ* method). This technique makes it possible to fill single-walled nanotubes with virtually any chemical compounds from the gas or liquid phases (depending on the aggregate state of the compound that is intercalated at the moment of contact with carbon nanotubes).[14] This approach is implemented in several steps the first of which is the opening of SWNT ends.§

Filling NTs from the liquid phase is often referred to as the capillary method. It is used for the introduction of suspensions, solutions or melts of low-melting compounds into nanotubes. The capillary effect requires a liquid (suspension, solution or melt) to interact with the solid surface of the nanotube walls, *i.e.*, the liquid phase must wet well the channel surface. Important parameters of the *ex situ* methods are the solubilities, melting points and decomposition points of compounds to be intercalated as well as the diameter of an SWNT. In addition, experiments should be carried out in vacuum since nanotubes are as a rule filled with absorbed gas molecules.[14]

1. Opening nanotube ends

The first step of the *ex situ* methods for filling carbon nanotubes is usually opening their ends, which can be carried out in two main ways,[14, 56] *viz.*, thermal treatment of NTs in an oxidative gaseous medium (dry air or oxygen) and treatment with liquid oxidants, such as concentrated acids (HNO_3, H_2SO_4, $HNO_3-H_2SO_4$), hydrogen peroxide, potassium permanganate, osmium tetroxide or a mixture $HF-BF_3$.[43, 48, 56–59] Concentrated acids are also used for removing catalytic particles and various contaminants (amorphous carbon, polyaromatic compound and graphite particles).

It is known that the graphite hexagonal lattice is extremely stable against chemical treatment. Only the carbon atoms of five-membered rings of fullerene hemispheres undergo oxidation, while the carbon atoms of six-membered rings of nanotube walls remain nearly unaffected. Thus, oxidants initiate the destruction of nanotube ends in the first step and then oxidize NTs from the opened ends with concomitant shortening of the nanotubes.

Actually, not only the ends, but also the walls of nanotubes undergo oxidation. Thus treatment of single-walled nanotubes with an acid resulted in the formation of lateral defects (one defect per 5 nm of the nanotube length).[35] Unlike multi-walled nanotubes, single-walled nanotubes form 'hole' defects upon partial oxidation, which allows penetration of a substance into the tubes not only through their ends, but also through their side surfaces.

A comparison of various methods for opening SWNTs showed that the opening of nanotubes occurs more efficiently on thermal oxidation than on treatment with acids.[26] Given that reduction products of acids can react with carbon atoms of SWNTs, the use of gaseous oxidants for nanotubes is preferrable in order to avoid the material contamination.[14, 56] Oxidation in air at 300–500 °C for ~30 min can be regarded as the optimum conditions. In this case, virtually complete opening of nanotubes takes place. This process is accompanied by ~40% loss of the sample mass.[35] A number of investigators believe that the oxidation of NTs requires a strictly constant temperature, namely, 420 °C. Smith and Luzzi[60] employed heating in vacuum at 225 °C for 63 h for opening NTs before their filling with fullerenes. However, the efficiency of this method for opening SWNTs proved to be very low as regards introduction of other compounds into nanotubes. Oxidation of single-walled nanotubes with a mixture of concentrated H_2SO_4 and HNO_3 (in the ratio of 3:1)

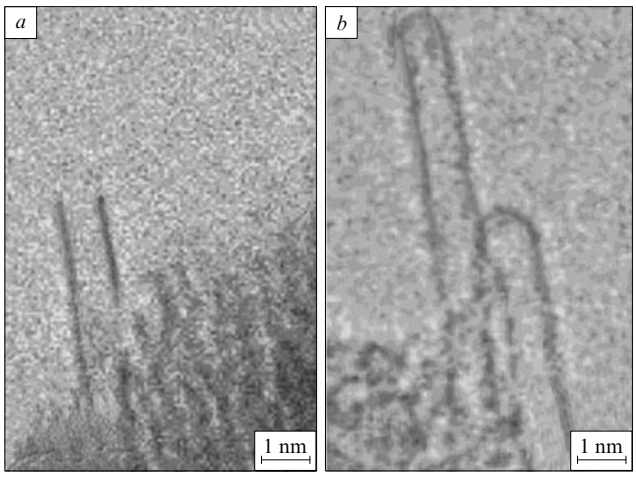


Figure 4. Single-walled nanotubes with opened ends after annealing at 400 °C for 10 h under vacuum (*a*) and the same tubes with closed ends after additional thermal treatment at 800 °C for 1 h (*b*).[61]

§ In most cases, SWNT ends are closed with hemispherical caps (fullerene hemispheres) that contain, along with six-membered carbon rings, five-membered rings in which the configuration of carbon atoms is less stable.

followed by thermal treatment at 400 °C for 10 h at 5×10^{-6} Torr leads to efficient and homogeneous opening of both ends of nanotubes (Fig. 4 *a*). Additional annealing of the obtained NTs in vacuum at 800 °C for 1 h results in the closure of the NT ends with fullerene hemispheres (Fig. 4 *b*).[61]

2. Filling single-walled nanotubes from the gas phase

Abundant examples of filling multi-walled nanotubes from the gas phase are known, while the data on filling SWNTs are scarce.[14, 62] Filling carbon nanotubes from the gas phase is performed, as a rule, in vacuum at high temperatures.[14] A sealed tube is heated up to the vaporization (or sublimation) temperature of an introduced material or somewhat higher.[14] The syntheses of '1D-crystal@SWNT' nanocomposites should be carried out at the lowest possible temperatures to minimize the reverse process (deintercalation). During annealing of the NTs, drawing (capillary condensation) of vapour of the compound to be intercalated into the nanotube takes place and its crystallization occurs on subsequent cooling of the system.

The two-step technique described is most often used for filling carbon nanotubes with fullerenes (for instance, C_{70}, with the sublimation temperature ~1520 K, Fig. 5), which have high affinities for nanotube surfaces and high vapour pressures (of the order of 3×10^{-4} Torr at 500 °C).[60, 63] According to the literature data, the intercalation of fullerenes occurs through the ends and wall defects of SWNTs. The intercalation process is strongly dependent on the temperature and time of NT treatment and to a lesser extent on the partial vapour pressure of the introduced compound.[60] This process is lengthy (~2 days), but enables homogeneous and complete (virtually 100%) filling SWNTs.

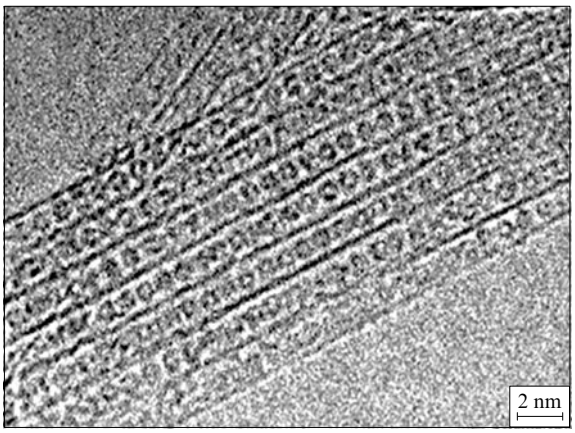


Figure 5. HRTEM micrograph of SWNT bundles filled with C_{70} fullerenes from the gas phase at 500 °C (24 h).[60]

Filling SWNTs from the gas phase is successfully applied to intercalate not only fullerenes, but also endofullerenes ($M_x@C_n$) or doped fullerenes.[14, 64, 65] Endofullerenes are, as a rule, preliminarily synthesized by the arc-discharge method with addition of a metal to the graphite anode (for instance, Gd for the preparation of $Gd@C_{82}$).[65] Then a mixture of open¶ SWNTs and endofullerenes is annealed at 400 – 500 °C in an evacuated tube at 200 °C for several days.[65] Using this method, SWNTs filled with a variety of fullerenes (C_{60}, C_{70}, C_{80}, C_{84}, C_{78}, C_{90}), doped fullerenes (Cs, K, $FeCl_3$) or endofullerenes ($N@C_{60}$, $La_2@C_{80}$, $Sc_3N@C_{80}$, $Er_xSc_{3-x}N@C_{80}$, $Dy_3N@C_{80}$, $Gd@C_{82}$, $La@C_{82}$, $La_2@C_{82}$, $Dy@C_{82}$, $Sm@C_{82}$, $Sc_2@C_{84}$ @ $Gd_2@C_{92}$) were obtained.[14, 66, 67]

The filling mechanism of nanotubes with compounds that do not possess high affinities for graphite, for example, Se, $ZrCl_4$ or Re_xO_y, is somewhat different from that described above. In this case, intercalation occurs according to the mechanism of capillary condensation of material in small-diameter pores (Figs 6 and 7).[26, 62, 68] Therefore, the compound to be introduced should possess high partial pressure at the synthesis temperature so that the compound vapour condensed in pores of nanotubes (channels) on cooling the system. Such a process is of small duration. The efficiency of filling SWNTs with materials with high vapour pressures (for instance, Se) is by far higher than that with fullerenes.

Figure 6 depicts transmission electron microscopy (TEM) image of a single-walled nanotube bundle containing small clusters of Re_xO_y. Non-uniform filling of SWNTs with Re_xO_y particles is seen, they are no more than 2 – 3 nm

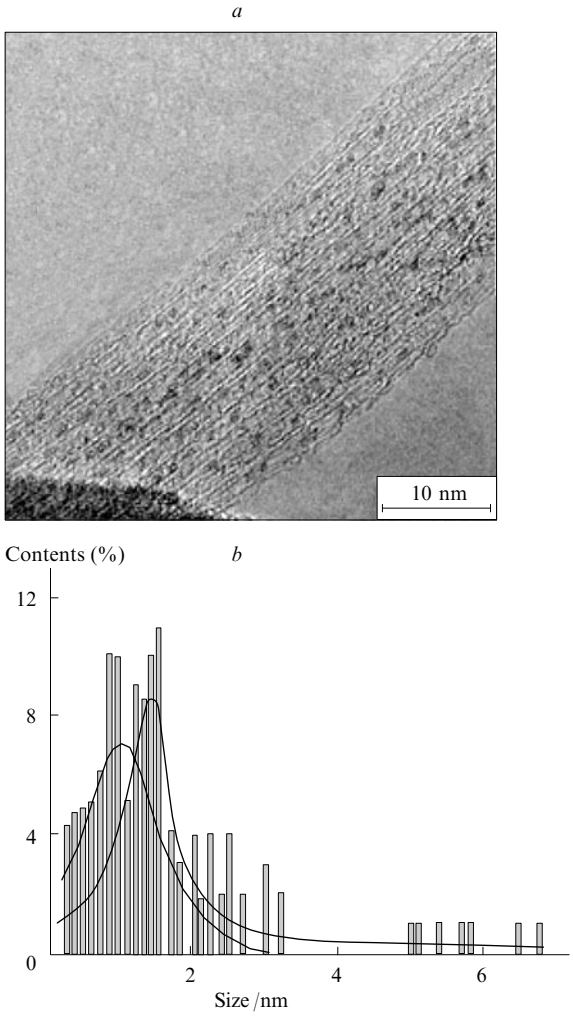


Figure 6. HRTEM image of a bundle of SWNTs filled at 250 °C with Re_xO_y clusters (*a*) and their size distribution (*b*).[68]

¶ In order to open SWNT ends, it is necessary to oxidize SWNT at 450 °C for 30 min in a flow of dry air.

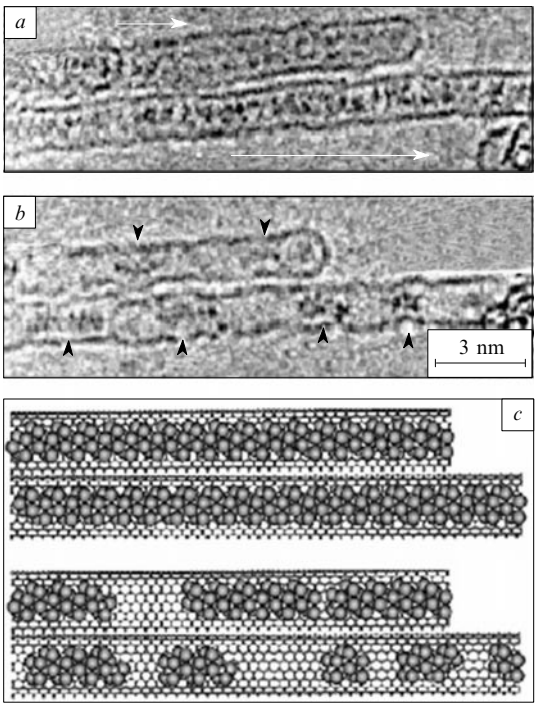


Figure 7. HRTEM images of SWNTs filled with $ZrCl_4$ chains (*a*) and individual $ZrCl_x$ nanoparticles (*b*) ~1 nm long after 4 min irradiation with an electron beam;[26] (*c*) an idealized representation of cluster formation within SWNTs depicted on microphotographs 7 *a*,*b*.

long. A procedure for filling single-walled nanotubes with chains of $ZrCl_4$ formed upon $ZnCl_4$ sublimation at 350 °C was reported[26] (Fig. 7 *a*). It was demonstrated that on irradiation with an electron beam the lengthy $ZrCl_4$ nanoparticles gradually disintegrate into discrete clusters of up to 3 nm length, which upon exposure for 4 min are segregated into $ZrCl_x$ nanoparticles that are ~1 nm long (Fig. 7 *b*,*c*).

The main drawback of the method considered is a limited choice of compounds that can be intercalated. First, its vaporization (or sublimation) temperature should not exceed 1000 °C to avoid its interaction with carbon and closure of the nanotube ends.[14] Second, this compound (as a rule, a volatile oxide or a salt) should be sublimed without decomposition. Another serious limitation of the method is the formation of discrete cluster particles, whereas the practical use of the composites requires continuous filling of nanotubes.

3. Filling single-walled nanotubes from the liquid phase

Filling SWNTs from the liquid phase is carried out using the so-called capillary method, which consists of impregnation of open nanotubes with solutions or melts of selected compounds.[35,45] The use of melts is preferable since this rules out contamination of composites with the solvent and also eliminates the filtration step leading to densification of the formed nanocomposite. The excess of the intercalated compound that remained on the outer surface of an SWNT can be removed by washing the sample or heating in dynamic vacuum.

Filling SWNTs from the liquid phase is a multi-step process (2–4 steps). The composites obtained in this way often undergo further modification, such as annealing at high temperatures, photolysis, irradiation with the electron beam, chemical or thermal reduction (or oxidation) to form nanoparticles of metals or their oxides in SWNT channels.[35,69,70]

Filling SWNTs from the liquid phase is of both practical and theoretical interest, since it allows receiving an experimentally substantiated answer to the question of what are the minimum sizes where capillary phenomena retain their pecularities. Thus it was theoretically predicted and experimentally proven afterwards that the capillary phenomena hold not only in the micro-, but also in the nanometre range.[71,72] The efficiency of filling SWNTs from the liquid phase depends on the surface tension (γ) of the liquid that fills SWNT, which determines the capillary pressure related to curvature of surface by the Young–Laplace equation

$$\Delta P = \frac{2\gamma\cos\theta}{r},$$

where r is the radius of curvature, θ is the wetting angle, ΔP is the pressure difference across the liquid–vapour interface. It was experimentally shown[71] that the surface tension of liquids should not exceed 100–200 mN m^{-1} in order to fill multi-walled nanotubes with diameter of 2–20 nm, which illustrates the role of capillary forces in the mechanism of substance impregnation into the channels of carbon nanotubes. Later,[73] the surface tension of liquids necessary for wetting surfaces of single-walled nanotubes was determined as 130–170 mN m^{-1}. The difference between the obtained values of surface tension is, seemingly, explained by smaller diameters of SWNTs (1.4–2.4 nm) in comparison with those of MWNTs and, consequently, higher surface curvatures of single-walled nanotubes.

When using the *ex situ* method for filling SWNTs from the gas phase, of great importance are (i) the viscosity of the liquid material, which affects the kinetics of filling nanotubes; (ii) the vapour pressure of the liquid to be intercalated, which allows the assessment of the possibility of the vapour intercalation into SWNT along with the liquid and, finally, (iii) the SWNT diameter. The latter determines not only the nanotube radius of curvature and therefore the surface tension of the material that can be introduced, but also the size limit of the intercalated objects. Recent investigations demonstrated that there are restrictions on the dimensions of SWNTs (a minimum diameter) for successful filling nanotubes with liquid phases.[74] Thus for the introduction of a V_2O_5 melt the surface tension of which equals 80 mN m^{-1} the diameter of an SWNT should be no less than 0.7 nm, while the critical diameter for $AgNO_3$ melt is 4 nm.[74,75]

Therefore, the retraction of a liquid into single-walled nanotubes requires that a number of conditions be met.[35] First, carbon nanotubes must be open from at least one end. Second, the liquid phase must effectively wet the SWNT surface, *i.e.*, its surface tension should not exceed 130–170 mN m^{-1}. This excludes the possibility of filling SWNTs with the melts having high surface tensions,† but allows the use of the majority of organic and inorganic solvents including water (γ = 72 mN m^{-1} at 25 °C) and benzene (γ = 28.9 mN m^{-1}). Third, the melting (decompo-

† For the encapsulation of substances with high γ values (for instance, metals), high pressures (several kbars) are to be employed in the synthesis.[59]

sition) points of the filling material should not exceed 1100 °C in order to prevent closure of a fullerene hemisphere and SWNT destruction in the composite syntheses.

The filling temperature for SWNTs is chosen depending on the chemical composition of compounds that are to be intercalated, their oxidizing ability, the quality of SWNTs used, *etc*. In the absence of effective interaction between the compound to be intercalated and the nanotube, the maximum synthesis temperature is limited to the temperature at which closure of a fullerene hemisphere takes place. Depending on the quality of the tubes, the T_{max} ranges from 800 to 1200 °C. It should be taken into account that the treatment of SWNTs at temperatures above 800–900 °C in an oxidizing medium leads to numerous defects in carbon nanotubes and their further destruction.

a. Intercalation from suspensions or solutions

Filling nanotubes with a suspension of nanoparticles in a liquid (solvent) implies the impregnation of open SWNTs, usually at room temperature.[14] In this case, evaporation of the solvent occurs both during and after the impregnation of nanotubes. This method is sufficiently efficient and straightforward, though it has some limitations associated with the sizes and morphologies of original nanoparticles. The diameters of nanoparticles that are to be incorporated should not exceed the internal diameter of a nanotube, the particles should be spherical, and their size distribution should be sufficiently narrow for most homogeneous filling of channels. Currently, filling nanotubes with suspensions of nanoparticles‡ is only exploited for multi-walled nanotubes, since particles with diameter more than 1 nm are regarded as unsuitable for filling SWNTs.[76] It is ferromagnetic nanoparticles that are basically employed for the filling. Preparation of suspensions of nanoparticles with diameter $\leqslant 1$ nm is a sufficiently complex process. The only known example[77] of filling single-walled nanohorns with Gd particles with diameter of 1 nm is an exception.

Filling nanotubes from solutions was developed in 1994. For the first time, it was applied to the synthesis of NiO and UO_{2+x} nanoparticles inside multi-walled nanotubes, and more recently to filling MWNTs with particles of Ag, Au, Pt, Pd , *etc*.[37,58,59] Several years elapsed until a research group from the University of Oxford headed by Sloan[78] employed this approach for filling single-walled nanotubes with Ru nanoparticles. To this end, SWNTs opened in concentrated hydrochloric acid were impregnated with a saturated solution of $RuCl_3$ in hydrochloric acid at 35 °C (5 h), then dried at 60 °C for 12 h and reduced in a stream of H_2 at 45 °C (3 h). Micrographs obtained by HRTEM and data from energy dispersive X-ray microanalysis of the composites confirmed the formation of ruthenium nanoparticles and elongated partially oxidized Ru clusters inside the SWNTs. The *d*(101) lattice fringes of ruthenium nanoparticles were oriented parallel to the SWNT axis.

At present, aqueous solutions of metal chlorides or nitrates (for instance, $RuCl_3$ or $AgNO_3$) are used most often for filling SWNTs from the liquid phase by the *ex situ* method.[35,37,45] Nitric acid having low surface tension (43 mN m^{-1}) is also used as a solvent,[51] which allows one to avoid the step of nanotube opening.[35,79] Hydrochloric acid and chloroform were used as solvents for the introduction of CrO_3 and Ru[78,80] and of $MoCl_5$ and $FeCl_3$,[14,45] respectively. In the second step, SWNTs filled with metal salts undergo as a rule thermal treatment or hydrogenation in a stream of hydrogen at 150–450 °C for several hours in the course of which nanoparticles of metals or their oxides are formed inside SWNTs.

Over the last decade, the approach described has successfully been applied to filling SWNTs with Bi, Ag, Au, Pt, Pd, Ru and Ru_xO_y, Fe nanoparticles that are 2 to 100 nm long on average.[13,14,45,51] Figure 8 shows micrographs of single-walled nanotubes filled with Bi, Pt and Au nanoparticles that are manufactured upon impregnation of SWNTs with solutions of $Bi(NO_3)_3$, $H_2PtCl_6 \cdot 6H_2O$ and $HAuCl_4 \cdot x H_2O$, respectively, followed by their reduction at 350–450 °C.[45,51] According to the data from HRTEM, the lattice spacing in the obtained Bi nanocrystals is equal to 0.33 nm, which corresponds to the interplanar spacing $d_{(012)}$ in the bulk bismuth crystal (Fig. 8 *a*), while in the Au nanoparticles $d = 0.23$ nm, which is in good agreement with the interplanar spacing $d_{(111)}$ in the bulk gold crystal (Fig. 8 *c*). Such a coincidence provides evidence for the absence of considerable deformations of the nanocrystals in the SWNT channels (see Section IV).[45,51]

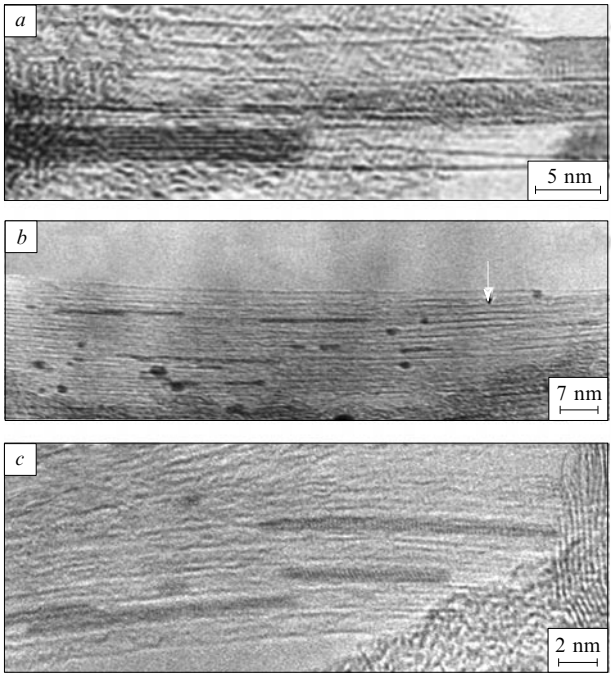


Figure 8. HRTEM micrographs of SWNT bundles of filled with single-crystalline Bi particles from the liquid phase with the lattice spacing $d_{(012)} = 0.33$ nm and length of filling ranging from a few nanometers to a few hundred nanometers (*a*),[51] with polycrystalline Pt particles with length in the range 3–20 nm (*b*) and with single-crystalline Au particles with $d_{(111)} = 0.23$ nm and length in the range 2 to 70 nm (*c*).[45]

An original technique for filling SWNTs with chromium oxide CrO_x was reported by Mittal *et al*.[80] As-prepared nanotubes (the arc-discharge method) were treated with a mixture of HCl and CrO_3 (in the molar ratio of 1 : 2) in open air for a long time (from 3 h to 1 month). Examination of the obtained samples by TEM and energy dispersive X-ray microanalysis after washing and drying demonstrated the presence of not only elements C, Cr and O, but also some Cl

‡ It should be noted that commercially available suspensions [for example, ferrofluids (Ferrotec, Japan)] contain nanoparticles with an average size of 10–100 nm.

in the nanotube bundles. Therefore, the following mechanism of filling nanotubes was suggested. Presumably, a strong oxidant CrO_2Cl_2 is formed first, which oxidizes nanotubes and opens their ends. This enables the chromium oxide CrO_3 (together with CrO_2Cl_2) to enter the SWNT channels.

$$CrO_3 + 2\,HCl \longrightarrow CrO_2Cl_2 + H_2O,$$

$$2\,CrO_2Cl_2 + Cl_2 + 2\,C \longrightarrow 2\,CrCl_3 + 2\,CO_2.$$

(The appearance of Cl_2 is associated with the photolytic decomposition of CrO_2Cl_2.)

According to the data from HRTEM, ~25% of the channels are filled with nanoparticles that are 4 to 20 nm long and devoid of a pronounced crystal structure (Fig. 9 *a*,*b*). However, a TEM image of a cross section of a filled nanotube shown in Fig. 9 *c* permitted the authors to assume the formation of three linear chains of the CrO_4 tetrahedra with threefold symmetry that are bound by van der Waals forces and located parallel to the SWNT channels.

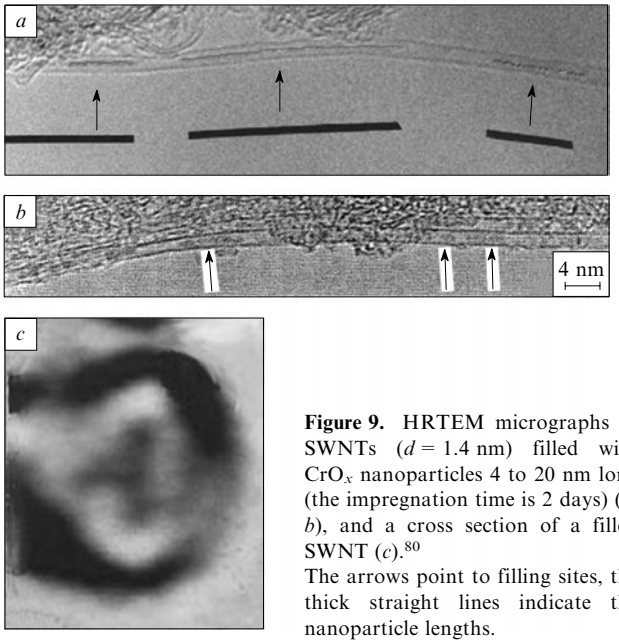


Figure 9. HRTEM micrographs of SWNTs ($d = 1.4$ nm) filled with CrO_x nanoparticles 4 to 20 nm long (the impregnation time is 2 days) (*a*, *b*), and a cross section of a filled SWNT (*c*).[80]
The arrows point to filling sites, the thick straight lines indicate the nanoparticle lengths.

Subsequently, the insertion of inorganic compounds into nanotubes from solutions was applied for the preparation of nanoparticles of more complex compositions.[37]

For this purpose, MWNTs were impregnated with $Fe(NO_3)_3$, $Cd(NO_3)_2$ or $AuCl_3$ solutions, after which the composites obtained were treated with a solution of $Bi(NO_3)_3$ or H_2S to yield $FeBiO_3$, CdS or Au_xS_y nanoparticles, respectively. The polycrystalline nanoparticles obtained in this way were 3 to 6 nm thick (corresponding to the internal diameters of MWNTs) and 3 to 30 nm long. Examples of filling single-walled nanotubes with complex compounds are unknown.

Other versions of the intercalation of substances into NTs from solutions are solvothermal synthesis and filling nanotubes from supercritical media. Both methods were successfully applied to the formation of nanoparticles of metals (Pd, Ni, Cu, Rh, Ru, Pt, Au), alloys (PtRu, PdRh, RuSn, $CoSb_3$), metal oxides (Eu_2O_3, Al_2O_3, Co_3O_4, CoO, Fe_2O_3, Mn_3O_4, ZrO_2, TiO_2, RuO_2), and also some polymers inside or on the external surfaces of multi-walled nanotubes.[81–86] However, attempts to intercalate inorganic compounds into SWNTs by these methods usually ended in failure.[84] The only instance of filling single-walled nanotubes from supercritical media is the intercalation of fullerenes and endofullerene $Er_3N@C_{80}$ into SWNTs from supercritical CO_2 or C_2H_4 at ~150 bar.[87]

From the examples cited above, one can see that the insertion of inorganic compounds into SWNTs from suspensions or solutions offers a broad range of possibilities for filling SWNTs with a wide variety of substances (metals, oxides, chlorides, fullerenes and endofullerenes). However, this method suffers from many shortcomings.[35] First, during the synthesis, contamination of the SWNT channnels with the solvent or its interaction products with the nanotube walls or with the intercalated compound is possible. Second, intercalation from solutions results in a heterogeneous distribution of a substance in an NT channel, and in addition, in incomplete (not 100%) filling of SWNTs, which pertains to the intercalation of solvent molecules into SWNTs. Indeed, the removal of the solvent or the formation of gaseous products in the thermal treatment leads to individual cluster particles 2 to 100 nm long, whereas the maximum filling yield is normally 25% – 30% (the lower the solution concentration of the compound to be intercalated the lower the degree of filling of the channels).[35] Let us also note that nanoparticles obtained by this method are most often polycrystalline, while of greatest practical interest is the formation of single-crystalline nanoparticles inside SWNTs.

b. Intercalation from melts

The problem of the continuous and uniform filling of SWNTs was successfully solved by the *ex situ* method of filling nanotubes from melts. This technique allows the filling yield of NTs to be 2 – 3 times larger as compared to the filling from suspension and solution.[14, 34, 36] The insertion of melts into single-walled nanotube channels due to capillary forces forms the basis of the method. The filling process is usually carried out in vacuum at temperatures that are 10 – 100 °C higher than the melting point of the material to be introduced, after which the filled NTs are slowly cooled down in order to crystallize the intercalated particles.[35] Metal halides and oxides as well as low-melting substances are used as a rule as the starting compounds, since they meet all requirements for materials to be intercalated, namely, they possess comparatively low surface tensions (below 170 mN m^{-1}) and melting points lower than 1100 °C (Table. 1).[14, 26]

For the first time, the *ex situ* insertion of melts into NT channels was used by Ajayan and Iijima (1993)[43] for filling multi-walled carbon nanotubes with PbO particles. They could reach a 90% filling yield, which is apporimately twice as high as the filling yield achived by other methods.[43] Later, Ajayan have demonstrated that this approach can succesfully be applied to fill SWNTs omitting the step of the preliminary opening of nanotube ends.[89] In 1999, Sloan *et al.*[69] employed the capillary technique for filling single-walled nanotubes with eutectic mixtures $(KCl)_x(UCl_4)_y$ and $AgCl_xBr_y$ with three different compositions: $x:y = 73.2:26.8$, 50 : 50 and 39.33 : 60.67 for $(KCl)_x(UCl_4)_y$ and $x:y = 100:0$, 20 : 80 and 0 : 100 for $AgCl_xBr_y$. The halide mixtures were ground together with an SWNT and sealed under vacuum in an ampoule, which was heated for

Table 1. Surface tension values and melting points of intercalated materials, synthesis temperatures of '1D-crystal@SWNT' nanocomposites (intercalation from melt), and also filling yields of nanotubes.[14, 25, 26, 88]

Material	γ /mN m^{-1}	T_{melt} /°C	$T_{intercal}$ /°C	Filling yield (%)	Material	γ /mN m^{-1}	T_{melt} /°C	$T_{intercal}$ /°C	Filling yield (%)
AgCl	113 – 173	560	560 – 660	40 – 50	KCl	93	771	870	–
AgBr	151	432	532 – 590	40 – 50	$(KCl)_x(UCl_4)_y$	44 – 65	335, 562	435, 662	< 10
$AgBr_{0.2}Cl_{0.8}$	173	410	510	40 – 50	KI	70	681	781	60 – 80
AgI	171	455	555	80 – 90	$LaCl_3$	109	860	910	20 – 40
Al	860	660	–	–	LiI	94	449	549	20 – 30
BaI_2	130	740	840	< 10	NaI	81	661	761	10 – 20
Bi_2O_3	200	825	–	–	$NdCl_3$	102	784	834	20 – 40
CaI_2	83	784	884	< 10	Pb	470	327	–	–
Cs	67	29	–	–	PbO	132	886	–	80 – 90
CsI	69	627	727	30 – 40	Re_2O_3	32	220	250	50 – 60
CuCl	–	430	530	30 – 50	Rb	77	39	–	–
CuBr	–	492	590	60 – 80	RbI	70	647	747	60 – 70
CuI	–	606	705	> 90	S	61	115	165	20 – 30
$EuCl_3$	–	850	860	20 – 40	Se	97	221	320	20 – 40
$FeCl_2$	–	674	774	–	Te	190	450	520	20 – 40
$FeBr_2$	–	684	784	–	$TbCl_3$	–	588	638	20 – 40
FeI_2	–	587	687	50 – 60	$SmCl_3$	–	686	706	20 – 40
Ga	710	30	–		UCl_4	27	590	690	< 10
$GdCl_3$	92	609	659	20 – 40	V_2O_5	80	690	–	–
Hg	490	– 38	–	–	$YbCl_3$	–	854	904	20 – 40
K	117	336	–	–	$ZrCl_4$	1.3	437	487	50 – 70

30 min at the temperatures about 100 °C higher than the liquidus or melting points of the filling material. The obtained samples were cooled at a rate of 3 – 5 deg min^{-1} and examined by HRTEM (Fig. 10). The TEM micrographs of the $(KCl)_x(UCl_4)_y$ samples point to the formation of single-crystalline nanoparticles $(KCl)_x(UCl_4)_y$ in SWNT channels (Fig. 10 *a*). Obtaining high-quality images of the $AgCl_xBr_y$@SWNT samples was complicated by the fact that silver halides are both light and electron beam sensitive (Fig. 10 *b*). The authors note an increase in the filling yield of nanotube channels from 20% to 50% in the series $AgCl < AgBr \leqslant AgCl_{0.2}Br_{0.8}$.

In single-walled nanotubes of large diameters (2 – 4 nm), spontaneous photolytic decomposition of AgCl was observed to form nanoparticles of metallic silver having a lattice periodicity of 2.04 Å (Fig. 10 *c*), which corresponds to the interplanar spacing $d_{(200)}$ in bulk silver (for comparison, AgCl is characterized by $d_{(020)} = 2.774$ Å). At the same time, the value of 2.04 Å agrees sufficiently well with the interplanar spacing $d_{(220)} = 1.962$ Å in bulk AgCl. In smaller-diameter nanotubes AgCl did not decompose; in this case crystalline particles of the $AgCl_xBr_y$ composition were produced in SWNT channels, which was confirmed by the data from energy dispersive X-ray spectroscopy. A possibility of filling SWNTs *ex situ* from a melt without a preliminary step of opening their ends was also pointed out, which can be accounted for by a selective interaction of carbon atoms of fullerene hemispheres with melts.

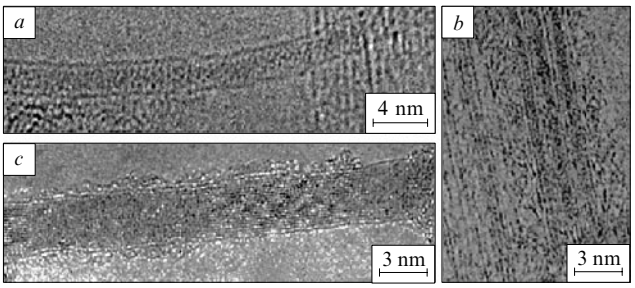


Figure 10. HRTEM images of SWNTs filled with a $(KCl)_x(UCl_4)_y$ eutectic mixture ($x:y = 73.2:26.8$) (*a*), AgBr particles (*b*) and Ag nanoparticles formed by photolytic decomposition of AgCl (*c*).[69] The $(KCl)_x(UCl_4)_y$@SWNT nanocomposite was obtained by filling the SWNT with a melt of KCl and UCl_4 at 662 °C for 30 min, followed by cooling for 3 h. The AgBr@SWNT nanocomposite was obtained by filling the SWNT with a melt of AgBr at 527 °C for 30 min followed by cooling for 3 h. The Ag@SWNT nanocomposite was obtained by filling the SWNT with a melt of AgCl at 560 °C for 30 min, followed by cooling for 3 h and photolytic decomposition of the salt.

By using the *ex situ* introduction of inorganic substances from a melt, SWNTs filled with nanoparticles of various metal halides [$M^{I}I$ (M^{I} = Li, Na, K, Cs, Rb, Ag), $M^{II}I_2$ (M^{II} = Ca, Cd, Co, Sr, Ba, Fe, Pb, Hg), $M^{III}I_3$ (M^{III} = La, Ce, Pr, Nd, Gd), $(Te/Sn)I_4$, Al_2I_6, $AgCl_xBr_yI_z$, $M^{I}Cl$ (M^{I} = Na, Cs, Ti), $M^{II}Cl_2$ (M^{II} = Cd, Fe, Co, Pd), $M^{III}Cl_3$ (M^{III} = La, Nd, Sm, Eu, Gd, Tb), $M^{IV}Cl_4$ (M^{IV} = Hf, Th, Zr, Pt), Al_2Cl_6, $(Th/V)Cl_6$], elements (S, Se, Te, I_2, Cs, Re, Bi, Pt, Au, Ru, Fe, Ag), fullerenes (C_{60}, C_{70}, C_{80}), endofullerenes ($Gd@C_{82}$), a mixture $(KCl)_x(UCl_4)_y$, oxides (Re_xO_y, V_2O_5, Sb_2O_3, CrO_3, PbO, UO_2), hydroxides (KOH, CsOH) and chalcogenides (SnSe, HgTe and $CdBr_{2-x}Te_x$) were synthesized.[14, 25, 34, 36, 45, 69, 71, 88, 90 – 97] HRTEM images of some SWNTs filled with inorganic compounds are provided in the Supplement (see the electronic version of this review at the journal's web-site http://www.uspkhim.ru).

Table 1 lists surface tension and melting points of some substances intercalated into SWNTs, and also filling temperature and filling yields.[14, 25, 26, 88] The conditions of filling nanotubes vary in different studies: thus heating rate ranged from 3 to 10 deg min^{-1}, the time of a sample exposure at the maximum synthesis temperature changed

within the limits 20 min to 6 h, whereas cooling rate did not exceed $1-5$ deg min^{-1}. In some instances, in order to achieve a high filling yield, nanotubes were exposed to contact with substances to be intercalated at the synthesis temperature for 20 h, and cooling was performed at the rate 0.1 deg min^{-1} to increase the crystallinity of nanoparticles.[45,97] According to the data from TEM, the filling yield of SWNT channels with inorganic compounds was 50% to 90% (see Table 1).

In most cases, the intercalated nanoparticles constituted one-dimensional nanocrystals (1D-crystals). Based on TEM images (Fig. 11 *a*), models of one-dimensional nanocrystals (Fig. 11 *d*,*e*) were developed, and also simulated TEM-images (Fig. 11 *b*,*c*) were obtained that were in good agreement with experimental ones. Nanocrystals differ substantially from bulk crystals in both their symmetry and bond lengths and bond angles. The distortions of geometric parameters are governed by steric limitation of a one-dimensional nanocrystal that is formed with nanotube walls and by adjustment of nanoparticle structures to the internal diameter of an SWNT channel. For example, in a nanocrystal of KI (2×2 atoms) interplanar spacing along the nanotube axis $d_{(200)} = 0.35$ nm (which corresponds to this distance in bulk KI), while in the direction that is perpendicular to the axis, it increases by 14% reaching the value of 0.4 nm (Fig. 11 *a*,*d*).[34,98]

Depending on the SWNT diameter, incorporated compounds (for instance, KI, PbI_2, HgTe) can produce distinct structures that differ in the number of atoms in a cross section of the tube or in symmetry.[34,96,97]

Nanocrystal structures simulated in several studies were compared with experimental HRTEM images of nanocrystals, which made it possible to verify the accuracy of the proposed models.[96,97]

In conclusion, it should be noted that the major advantages of *ex situ* filling from melt, apart from the possibility of filling SWNTs with a wide range of materials, are the relative simplicity of the method, the uniformity of prepared samples, high filling yield of nanotubes (up to 90%) and high crystallinity of obtained nanoparticles. A great merit is also the fact that the '1D-crystal@SWNT' systems are not contaminated with solvents and by-products (oxides, carbides). Thus, the *ex situ* filling of single-walled nanotubes from melt, considering all the presented parameters, is the most efficient of all currently existing approaches, which makes its utilization for the development of composites based on SWNTs most promising.

Nevertheless, filling SWNTs from melt is not applicable for compounds with surface tension values larger than 170 mN m^{-1} and melting points above 1100 °C. These limitations become a serious obstacle to direct introduction of many metals (due to high γ values of their melts) and covalently bound compounds [for instance, refractory metal oxides ($A^{II}B^{VI}$) and chalcogenides ($A^{IV}B^{VI}$)] into SWNT channels. However, it is the intercalation of metallic nanoparticles into semiconducting SWNTs that leads to the most significant changes in the electronic structures of single-walled nanotubes.[70,99–101] The broadband small-sized semiconductors $A^{II}B^{VI}$ and $A^{IV}B^{VI}$ with exciton diameter of several nanometers to tens of nanometers (for example, the diameter of small-sized CdS is 4.8 nm) are promising for both studying quantum-size effects and also using them as light emitters, sensors, solar cells, *etc*.[102] Several papers are devoted to studies on small-sized nanostructures $A^{II}B^{VI}$ and $A^{IV}B^{VI}$ obtained using carbon nanotubes as templates.[37,102–104]

It should be noted that filling nanotubes with refractory semiconducting materials by direct methods failed, hence it was decided to synthesize such materials in the internal channels of SWNTs.[105] To this end, first, nanotube channels were filled with molten metal iodides (ZnI_2, CdI_2, PbI_2) by the capillary method at the temperatures that were 100 °C higher than their melting points (M_p = 446, 388 and 412 °C, respectively). The MI_2@SWNT composites obtained underwent sulfidation, selenation or telluration by treating them with molten chalcogens:

$$MI_2@SWNT + 2X\,(liq) \longrightarrow \longrightarrow MX@SWNT + {}^1/_2 I_2\,(vap) + {}^1/_4 X_nI_m\,(vap), \quad (1)$$

$X = S, Te;\ X_nI_m = 2S_2I_2$ or Te_4I_4,

$$MI_2@SWNT + X\,(liq) \longrightarrow MX@SWNT + I_2\,(vap), \quad (2)$$

$X = Se$.

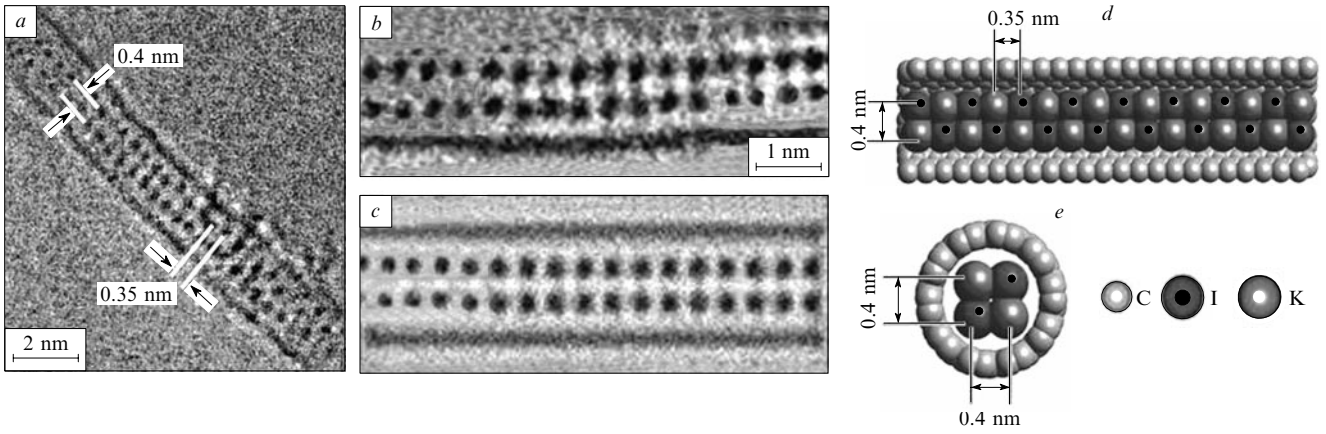


Figure 11. HRTEM image of a KI crystal (2×2 atoms) in an SWNT channel (1.4 nm in diameter) (*a*), simulated TEM images of the nanocomposite KI@SWNT (*b*, *c*) and its structural model (*d* is longitudinal section, *e* is cross section).[98]
The nanocomposite KI@SWNT was obtained by capillary filling of nanotube channels with diameter 1.4 nm, which were synthesized by arc-discharge technique, with molten KI at 651 °C for 30 min followed by cooling for 3 h.

Slow cooling of the chalcogenides produced in SWNT channels resulted in their crystallization to yield one-dimensional crystals. It was assumed [70] that the transportation of chalcogen atoms into cavities of single-walled nanotubes filled with the iodides MI_2 and the removal of the gaseous molecules of I_2 and X_nI_m produced in the reactions (1) and (2) occur through defects in SWNT walls. These data are in good agreement with the observed destruction of one-dimensional crystals in SWNT channels on irradiation with a beam of high-energy electrons [irradiation brings about escape of intercalated compounds through defects in the nanotube walls and decomposition on their external surfaces (see Section IV)].[27] The effectiveness of this approach (carrying out chemical reactions in SWNT channels) was exemplified by the synthesis of the semiconducting compounds $A^{II}B^{VI}$ and $A^{IV}B^{VI}$ (A = Zn, Cd, Pb; B = S, Se, Te) (Fig. 12), which possess high melting points (up to 1750 °C and the band gaps of 0.3 to 3.7 eV.[70]

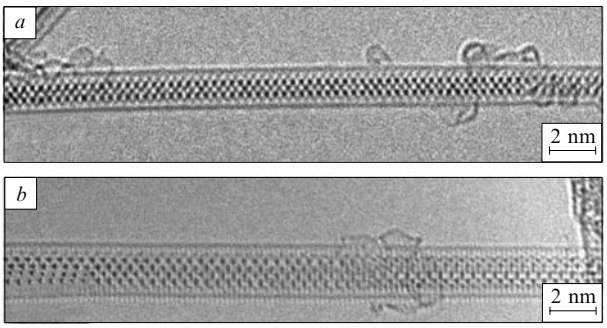


Figure 12. TEM-Microphotographs of the $PbTe_xI_{2-2x}$@SWNT composite (two types of observed projections).[70]

IV. Structures and properties of '1D-crystal@SWNT' nanocomposites

The '1D-crystal@SWNT' nanostructures are of tremendous interest from both theoretical and applied viewpoints. This branch of research has been developed for less than 10 years, therefore, the number of works on the unsual '1D-crystal@SWNT' composites is not large.[14] Even more rare are studies that address the simulation of structures and electronic properties of filled carbon nanotubes (see Refs 29, 100, 101, 106). The interest of experimentalists in such composites is associated with the possibility of altering the band gaps of SWNTs owing to filling the latter with electron-donor or electron-acceptor compounds and also with the possibility of changing the atomic and electronic structures of intercalated compounds due to forced structural deformations of material within single-walled nanotubes.[99]

The most efficient research tool for studying '1D-crystal@SWNT' nanocomposite structures is high resolution transmission electron microscopy (HRTEM). A '1D-crystal@SWNT' nanocomposite represents a single-walled carbon nanotube with a 1D-crystal inside. HRTEM images show either crystallographically ordered arrangement of atoms or columns of two or three atoms.

Inelastic scattering is the predominating process in the interaction of an electron beam with carbon atoms of a nanotube. Elastic scattering that pertains to the interaction of electrons with the atomic nucleus occurs mainly on interaction of an electron beam with a 1D-crystal. Radiation damages caused by elastic scattering increase with an increase in accelerating voltage and diminish with an increase in the mass of a nucleus. In order to reduce the radiation damages that can appear in the investigations of '1D-crystal@SWNT' nanocomposites, one has to decrease the accelerating voltage to 80 kV.§ This became possible by virtue of the use of a corrector of spherical aberration (C_s) and the reduction of chromatic aberration (C_c) through upgrading the electron microscope. In the study of a 1D-crystal, it is desirable that the intercalated inorganic compound contained at least one element with a high atomic number Z since the contrast in images of single atoms is proportional to Z^2.

HRTEM images of nanocomposites are categorized, analyzed and compared with the 3D-atomic structure of an intercalated compound. The comparison is used to choose crystallographic directions that presumably coincide with the SWNT axis. Of these directions those are selected that correspond to the images on micrographs in periodicity, cross-sectional dimensions and a structural motif. Then, taking into account atomic coordinates and scanning mode, a simulated image is obtained that is compared to the HRTEM image.

Historically first nanocomposite studied by HRTEM was the '1D-KI@SWNT' composite.[98, 107] It was found that KI crystals (3×3 atoms) are formed upon filling 1.6-nm-diameter nanotubes, while in nanotubes of a smaller diameter (1.4 nm), KI crystals (2×2 atoms) are incorporated. An increase in the parameters of the KI crystal lattice in the direction that is perpendicular to the tube axis was noted.

The simplest '1D-crystal@SWNT' nanocomposites are nanotubes filled with fullerene molecules (the so-called nanopeapods).[108] Depending on the ratio of the fullerene and NT internal diameters, a variety of 1D-crystals based on C_{60} are formed. If the internal diameter of an NT is less than 1.45 nm, linear chains of C_{60} molecules are formed, if the diameter is 1.45–2.6 nm, zigzag or spiral structures are produced, in tubes of a larger diameter up to four fullerene molecules can be accommodated in a tube cross section.[66, 109]

Examination of C_n@SWNT nanocomposites by transmission electron microscopy showed that fullerene molecules in SWNT channels move along a channel and coalesce. These observations initiated development of a whole branch of research on structural conversions of SWNTs filled with fullerenes, endofullerenes, doped or functionalized fullerenes.[14, 64, 65] Thus electron beam irradiation of C_{60} fullerenes close-packed in SWNT channels (accelerating voltage of 100 kV) first induced their dimerization followed by coalescence in the course of which an elongated capsule from C_{60} molecules is formed in the nanotube.[108] The coalescence is also observed on high-temperature (700–1200 °C) treatment of such structures. As a result, the formation of the second (internal) channel occurs in an NT and a double-walled carbon nanotube (DWNT) is produced.[108]

It should be noted that not only intercalated fullerenes undergo electron beam irradiation-induced transforma-

§ At the accelerating voltages 300–400 kV, both the nanotube walls and the one-dimensional crystal itself are destroyed.

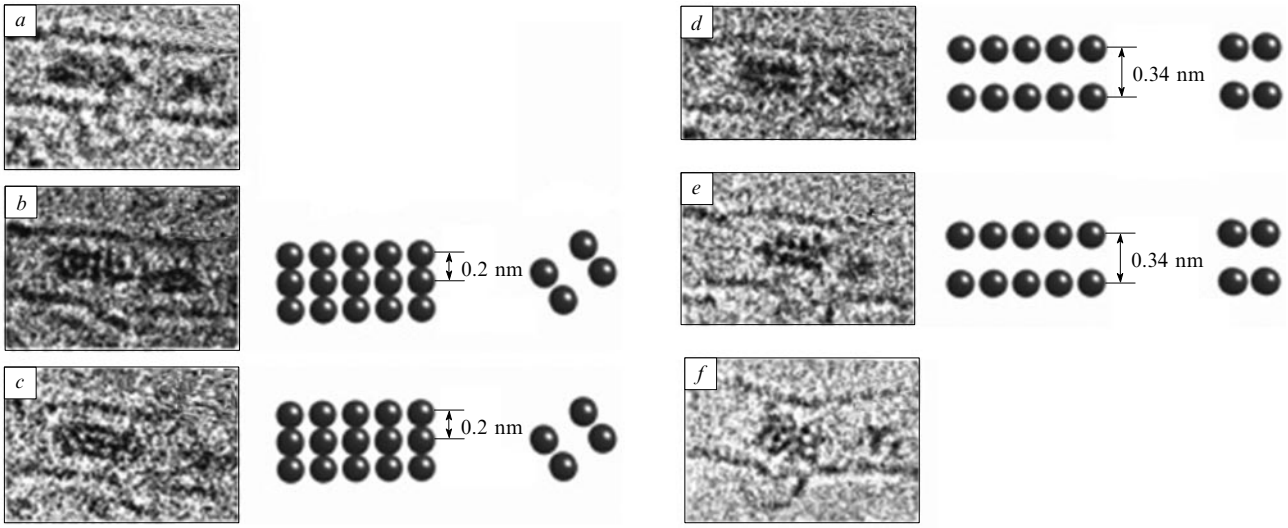


Figure 13. The behaviour of Re_xO_y clusters inside SWNT under the influence of the electron beam and a model representation of the clusters that demonstrates their rotation.[68]
Different projections of one cluster ($a-e$) and its image (f), which illustrates partial disintegration of nanotubes and the exit of the substance onto the surface, are shown.

tions, but also intercalated inorganic compounds. Thus dynamic behaviour of the $ZrCl_4$, Re_xO_y and CuI nanoparticles in SWNT channels on electron beam irradiation is reported.[26, 68, 110] The $ZrCl_4$ nanoparticles are clusterized (see Fig. 7 *b*,*c*), the Re_xO_y clusters evenly rotate inside single-walled nanotubes (Fig. 13), while one-dimensional crystals of CuI exit to the surface of a nanotube and decompose to yield metallic copper (see Fig. 17).

It is known that crystallization of a substance within single-walled nanotubes substantially changes its crystal structure and properties, and the structure of the one-dimensional nanocrystal formed proves to be metastable.[14] This was exemplified by nanoparticles of metal halides (AgBr, AgI, $CoCl_2$) that are nanowire-shaped within SWNT. After removal of the carbon shell, these particles lose the nanowire morphology.[111]

Deviations of 1D-crystal structures inside SWNT channels from the structures of the bulk materials have repeatedly been observed. Actually, these deviations pertain to changes in the crystallographic orientation of the nanocrystal with respect to the nanotube axis (the long axis of a one-dimensional nanocrystal can correspond to different crystallographic directions of the bulk substance); to reduction in the coordination number of atoms of an intercalated inorganic substance; to a change in the crysal lattice parameters of the one-dimensional crystal as compared to those of the bulk material, and also to the formation of nanocrystals with a crystal lattice that is not characteristic of bulk materials.[14, 34]

The change in the crystallographic orientation of the nanocrystal relative to the nanotube axis arises from the demand for the highest possible retention of the stoichiometry of the intercalated compound,[36] whereas the reduction in the coordination number of atoms and the change in the crystal lattice parameters of the nanocrystal along a radial direction, obviously, result from the spatial confinement of the nanocrystal by the SWNT walls.[34, 36, 80] The nanocrystal lattice parameters along the nanotube axis are less distorted, since in this direction there are virtually no steric limitations. Nevertheless, a number of studies point to the compression of the crystal lattice of the1D- crystal along the SWNT axis. In particular, this is typical of the Ag, Sb_2O_3, KI nanocrystals and $(C_{60})_n$ fullerene chains.[14, 112, 113] The observed lattice distortion can reach 14%. The compression (or stretching) of a crystal lattice parameter along the nanotube axis seems to be connected with a stretching (or constriction) of the unit cell of the SWNT channel in a radial direction; the cell volume is retained on such alterations.

Bulk metal halides are characterized by diverse types of crystal structures (including three-dimensional, layered, chain-like or molecular, Table 2). However, in the confined space of SWNT channels many of these structures cannot develop (this especially applies to the three-dimensional and layered structures, see Table. 2).[14, 34] Depending on the ratio between a crystal lattice parameter of the incorporated compound and the internal diameter of the SWNT channel, both the degree of crystallinity and crystal structure of the one-dimensional nanocrystal being formed in the nanotube channel can change. Thus for the CuHal@SWNT and AgHal@SWNT (Hal = Cl, Br, I) systems, the degree of crystallinity of nanoparticles inside the SWNT channels increases on going from the metal chloride to iodide, which is assumed to relate to the increase in the radius of the halogen ion when moving from Cl to I [$r_{(Cl^-)} = 1.67$, $r_{(Br^-)} = 1.82$, $r_{(I^-)} = 2.06$ Å], and consequently, to the increase in the M–Hal bond lengths in this series.[105] Thus in the CuCl@SWNT composite the CuCl single crystal fills the internal channel of the nanotube incompletely, resulting in sufficient mobility of Cu and Cl atoms, which leads to a decrease in the degree of crystallinity of the single crystal, while in the CuI@SWNT composite the size of the CuI crystal exactly fits the diameter of the tube, and so the degree of crystallinity increases. It should be noted that for some composites (for example, for CuI@SWNT and PbI_2@SWNT) a change in the structural type of the nanocrystal upon variation in the nanotube diameter was observed.[97, 110]

Let us consider the results of an HRTEM investigation of the 1D-CuI@SWNT nanocomposite in more detail.[110]

Table 2. Structural types of metal halides in M_nX_m@SWNT nanocomposites and in bulk crystals.[34]

Halide	Structural type of a bulk crystal	The coordination number of a metal in the bulk crystal	Structural type of a halide in the nanocomposite	The coordination number [a] of a metal in the 1D-crystal
KI	3D-halite	6	3D-halite	4, 5, 6
CuI	"	6	"	4, 5, 6
AgX (X = Cl, Br, I)	"	6	"	4, 5, 6
	wurtzite	4	wurtzite	3, 4
CsX (X = Cl, Br, I)	3D-halite	6	3D-halite	4, 5, 6
	BCC	8	BCC along [100]	4, 6, 8
SrI_2	3D-framework	7	1D-polyhedron chain	4, 6, 8
BaI_2	"	7 + 2	the same	5, 6
UCl_4	"	8	"	6, 8
$ThCl_4$	"	8	"	6, 8
TeI_4	"	8	"	6, 8
$LnCl_3$ (Ln = La – Tb)	"	8 + 1	"	6, 8
HgI_2 (red)	2D-layers	3	"	2, 3
PbI_2	"	6	"	5, 6
CdI_2	"	6	"	5, 6
$CdCl_2$	"	6	"	5, 6
$LnCl_3$ (Ln = Tb – Lu)	"	6	"	5, 6
$ZrCl_4$	1D-chain	6	"	6
$HfCl_4$	"	6	"	6
Al_2Cl_6	molecular	4	molecular	4
ZnI_4	"	4	"	4
WCl_6	"	6	"	6

[a] Observed or predicted.

The bulk (3D) CuI compound is an ionic conductor with iodide ions constituting close-packed hexagonal sublattice[114] in which copper cations occupy all tetrahedral interstices and a small part of octahedral interstices.

The HRTEM examination of the 1D-CuI@SWNT composite was initially carried out at the accelerating voltage 300 kV on a JEM 4000EX instrument (C_s = 0.9 mm). As a result, several types of 1D-CuI images were obtained. Noticeable electron beam-induced damage of the SWNT walls occurs (Fig. 14 *a*). In the re-examination of this nanocomposite at the accelerating voltage of 80 kV using a FEI Titan 80 – 300 instrument (C_s = 0.005 nm), destruction of the walls was insignificant (Fig. 14 *b*). Analysis of the obtained images allowed their separation into two groups dependent on the cation positions. Within each group, the images vary depending on the rotation angle (φ) of the axis of a nanotube relative to the electron beam. Two crystallograpic directions [001] and [1$\bar{1}$0] along which crystallizaton of CuI within the SWNTs could take place were selected in the 3D-crystal of CuI. For these two cases, atomic models have been constructed.

The atomic model of the 1D-$CuI_{[001]}$@SWNT composite with arrangement of copper cations in octahedral cavities is portrayed in Fig. 14 *d*. A side view of the model (φ = 0°) is illustrated in Fig. 14 *e*. The suggested atomic model served as the basis for obtaining a simulated image that takes into consideration atomic coordinates, atomic number and scanning parameters. The obtained simulated image (Fig. 14 *c*) corresponded to one of the most typical electron microsopic images of the 1D-CuI@SWNT nanocomposite (Fig. 14 *b*). On the latter, dark (with the focus of the electron beam $-\Delta f$) 'subunits' are clearly seen that are surrounded with white halos corresponding to projections of the columns of two iodine atoms, whereas single iodine atoms are zigzag-arranged. Copper cations are located in this projection near the SWNT axis, the periodicity of the structure $d_{[001]}$ = 0.72 nm agrees well with the 3D-structure of CuI, in which $d_{[001]}$ = 0.7186 nm.[115]

In the case of the location of copper cations in tetrahedral interstices one should allow for the fact that the ions vibrate in the holes, being in two possible positions. The residence time for a copper cation in one of the tetrahedral

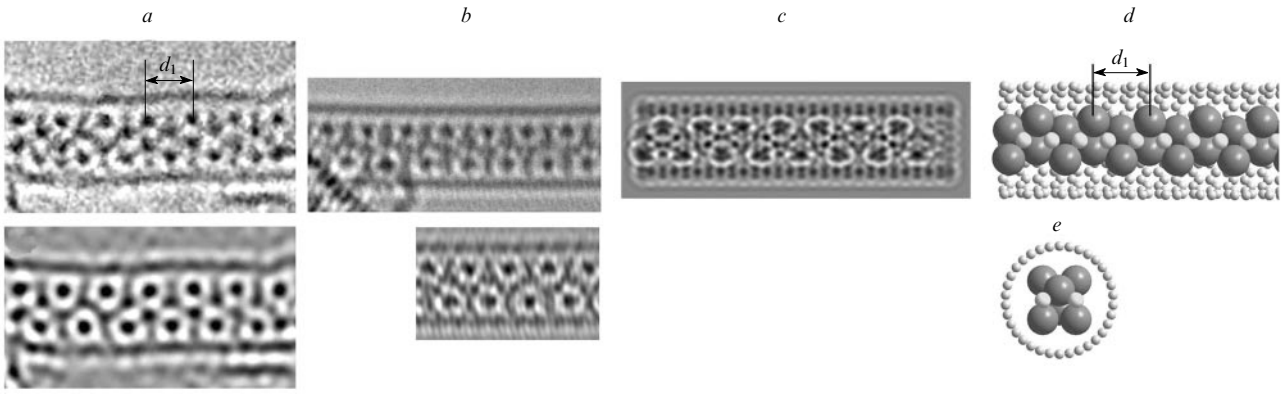


Figure 14. HRTEM Images of the 3D-$CuI_{[001]}$@SWNT nanocomposite with copper cations located in octahedral interstices;[110]
(*a*) the first type of images (φ = 0°) obtained at the accelerating voltage 300 kV [original (top) and filtered (bottom) images, d_1 = 0.72 nm]; (*b*) the same type of images obtained at the accelerating voltage 80 kV [original (top) and filtered (bottom)]; (*c*) simulated image for Δf = −15.6 nm; (*d*, *e*) atomic model of the 3D-$CuI_{[001]}$@SWNT compsite when copper cations are located in octahedral interstices [longitudinal (*d*) and cross (*e*) sections of the atomic model].

positions is 10 – 100 ps,[110] whereas the camera exposure time is 0.25 s. Accordingly, on a microphotograph Cu^+ cations appear in two tetrahedral interstices simultaneously. Presumably, such a structure matches the image type illustrated in Fig. 15 *a*. The corresponding atomic model and simulated images of the two nanotube ends for $\varphi = 0^\circ$ are portrayed in Fig. 15 *b*,*c*,*d*. Images corresponding to other projections of the nanocomposite were also analyzed.

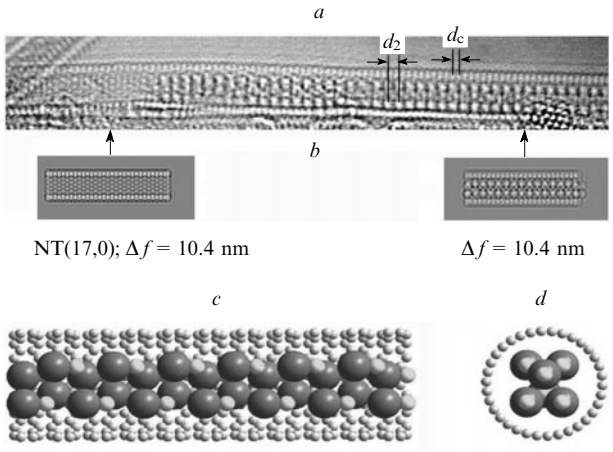


Figure 15. HRTEM images of the 3D-CuI$_{[001]}$@SWNT nanocomposite with copper cations located in tetrahedral interstices.[110, 116]
(*a*) is the first type of images ($\varphi = 0^\circ$, $d_2 = 0.36$ nm, $d_c = 0.2$ nm); (*b*) simulated images of the two NT ends (17,0) for $\Delta f = +10.4$ nm (on the left, the nanotube is empty; on the right, it is filled with CuI particles; an overlap (convolution function) of the images of nanotube walls is observed); (*c*, *d*) atomic model [longitudinal (*c*) and cross (*d*) sections].

In the case where the crystallization of CuI occurs within the internal channel along the crystallographic direction $[1\bar{1}0]$, other image types are formed.[110] It appears that there is certain correlation between crystallization direction and nanotube diameters. Crystallization in the direction [001] is observed in the nanotubes that are 1.32 ± 0.03 nm in diameter, while along the direction $[1\bar{1}0]$ it occurs in the nanotubes that are 1.41 ± 0.03 nm in diameter.

In the HRTEM study of the 1D-CuI@SWNT nanocomposite, two phenomena have been discovered: (1) the rotation and oscillation of the CuI crystal in the nanotube channel and (2) its exit from the nanotube through macrodefects.[27] For this nanocomposite, 50 images were obtained (selected images are depicted in Fig. 16). A small fragment of a CuI 1D-crystal (~ 5.1 nm long) is seen in the nanotube. The crystal moves and rotates. By the end of scanning, the crystal is destroyed. It was established that the movement of the crystal is due to the emergence of water vapour in the microscope column. Water molecules in a high-energy electron beam are ionized to yield O_2^- and OH^- ions. These ions interact with the SWNT walls to produce defects. If the quality of vacuum is improved, the movement of the crystals is considerably reduced.

In the case of a macrodefect in an SWNT wall (for example, a nanotube fracture, as shown in Fig. 17 *a*), the movement of a 1D-crystal is accompanied by its electron beam-induced destruction into individual CuI molecules. After molecules have escaped from the nanotube, iodine vaporizes, and copper atoms form clusters on the outer side

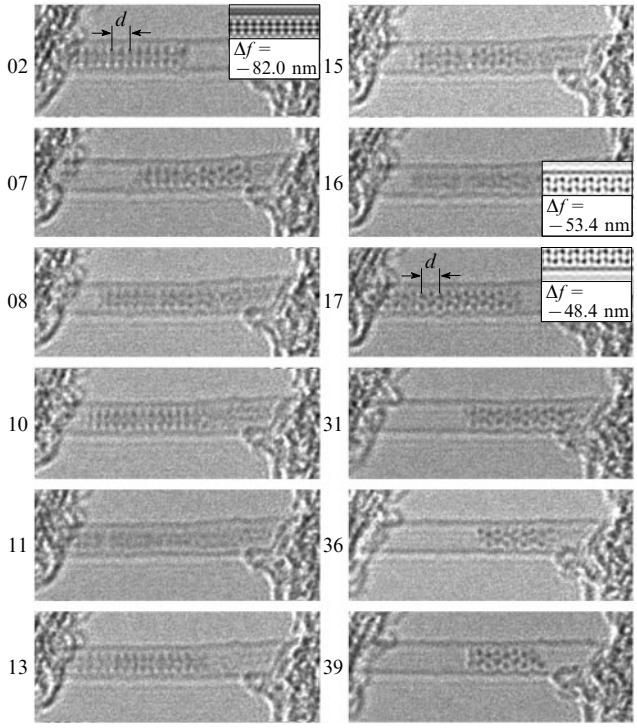


Figure 16. The oscillation and rotation of a 1D-CuI nanocrystal within SWNTs.[27]
50 Images per 25 s were obtained (the exposure of the CCD-camera was 0.5 s, accelerating voltage was 100 kV).

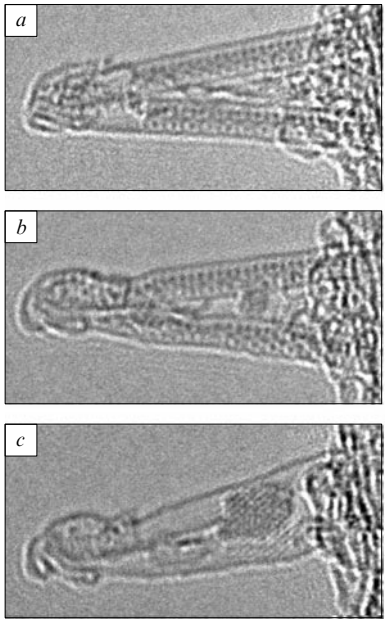


Figure 17. The exit of a CuI nanocrystal from an SWNT's internal channel through a macrodefect.[27]
(*a*) the beginning of electron irradiation (accelerating voltage is 100 kV), (*b*) the formation of a copper cluster, (*c*) the complete exit of CuI from the nanotube, the formation of a copper nanocrystal.

of the nanotube (conjecturally, cuboctahedra, see Fig. 17 *b*), which are then transformed into copper nanocrystals (Fig. 17 *c*). This process has been traced from the beginning to the end, which enabled estimation of the amount of copper ions that escaped from the nanotube and, based on the 1D-CuI model, its comparison with the amount of copper atoms in the nanocrystal. Good agreement was found. Thus, having 'metered' just hypothetically a nanocomposite of a definite length, a required amount of the atoms of copper or any other metals as a cluster or nanocrystals can be transferred to the required place.

The discussed method for modelling 1D-crystal structures is not unique. More advanced is the reconstruction of exit plane wave function from a series of shots taken with focus variation of an electron beam ('through focus'). Using this method, for instance, the structure of the HgTe@OCHT composite was determined.[96] However, considering the tendency of 1D-crystals to move and rotate in the internal channel of a nanotube, such a technique by far not always can be applied.

A series of micrographs made at 0.25 s exposure of a CCD-camera (Fig. 18) portray fullerene molecules within an SWNT where a 1D crystal of $PbTe_xI_{2-2x}$@SWNT is present simultaneously.[116] The nanotube filled with fullerenes is about 1.3 nm in diameter. Judging by distances between C_{60} molecules, individual molecules C_{60} are observed on the images (Fig. 18 *a*,*c*). The left-hand nanotube originally filled with fullerenes has a fracture (macrodefect) in the middle. Out of the fracture, the nanotube is also filled with fullerenes that have direct contacts with the one-dimensional crystal of $PbTe_xI_{2-2x}$. In the course of time, part of fullerene molecules coalesce to yield elongated structures of two or three molecules (Fig. 18 *b*). These molecular ensembles move along the nanotube channel together with the one-dimensional crystal.

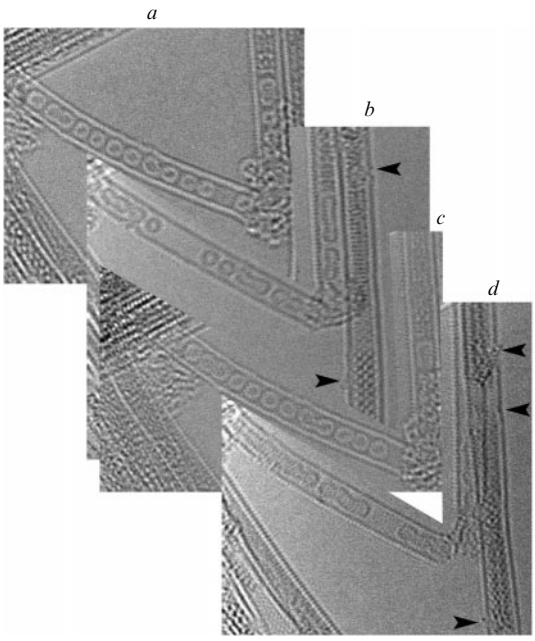


Figure 18. C_{60}@ SWNT and $PbTe_xI_{2-2x}$@SWNT nanocomposites.[116] (*a*) original image of the C_{60}+ PbTeI@SWNT nanocomposite with the focus of an electron beam $+\Delta f$; (*b*) images of C_{60}+PbTeI@SWNT (the left-hand nanotube) and PbTeI@SWNT (the right-hand nanotube) nanocomposites after 2.5 s with the focus $-\Delta f$ (defects in nanotube walls are designated with arrows). Co-motion of fullerene molecules and the one-dimensional crystal along the channel is observed. (*c*) Image of the C_{60}+PbTeI@SWNT nanocomposite after 4 s with the focus $+\Delta f$. Coalescence of fullerene molecules in the nanotube channel is observed. (*d*) Images of the C_{60}+PbTeI@SWNT (the left-hand nanotube) and PbTeI@SWNT (the right-hand nanotube) nanocomposites after 4.25 s with the focus $-\Delta f$. The distinct values of the focus ($\pm\Delta f$) of the electron beam are accounted for by vertical movement of the sample.

The right-hand tube (see Fig. 18 *b*) is filled with a one-dimensional crystal of $PbTe_xI_{2-2x}$. For the introduction of the one-dimensional crystal, a two-step method was employed according to which a nanocomposite of PbTe@SWNT was initially obtained and then treated with a solution of PbI. The crystal structure of 1D-PbTe was studied.[75] It was demonstrated that one of the modifications of this crystal is asymmetric in section. The presence of such a crystal in the NT channel imparts the shape of an ellipse to the nanotube. The nanotube deformation and its electron beam irradiation apparently contribute to the emergence of defects in a nanotube wall.

In a number of works it was shown that the crystallization of inorganic compounds within nanotubes depends, on the one hand, on the nanotube diameter, while on the other, on the ability of the SWNT wall for deformation. Indeed, it was found that SWNT walls of small diameters adjust to a nanocrystal structure (for example, in the CoI_2@SWNT and PbI_2@SWNT nanocomposites) as much as a filled nanotube adopts the shape of an oval in section.[92,97] It is interesting that PbI_2 particles incorporated into double-walled nanotubes with the same diameter as the single-walled remain amorphous. This is seemingly associated with considerably lesser deformability of DWNT walls as compared with that of SWNT, as a result of which PbI_2 does not crystallize.

Sometimes the spatial confinement of an intercalated substance by a channel wall can be so significant that a 1D-crystal with the structure that is not characteristic of the 3D-crystal of the same compound is produced. For instance, 3D-AgBr has a cubic lattice,¶ whereas the 1D-crystal formed within an SWNT has a hexagonal structure that is absent from the phase diagram of the bulk crystal.[118] In a number of cases, the formation of entirely new structures was observed that possess unusual properties including fivefold symmetry (see Fig. 9 *b*).[72,80,88,92,119]

It is of note that all the described structural pecularities of one-dimensional nanocrystals are manifested only when the crystals are formed within single-walled NTs. In filling multi-walled nanotubes of a considerably larger diameter, these pecularities do not appear.

V. Investigations into functional properties of '1D-crystal@SWNT' composites

The structural pecularities of '1D-crystal@SWNT' composites are manifested in their unusual physical properties, especially in their magnetic and transporting properties.[120] It was demonstrated[121] that the electrical conductivity of I_2@SWNT composites increases in comparison with that of pure nanotubes virtually by two orders of magnitude, which is presumably due to charge transfer from nanotube walls to

¶ The hexagonal structure of 3D-AgBr was found only at high pressure.[117]

iodine nanoparticles that possess electron-acceptor properties. This results in the generation of a large amount of charge carriers (holes) in semiconducting nanotubes and a descrease in SWNT resistance. It should be noted that in the I_2@SWNT systems involved, I_2 molecules occupied the space between nanotubes rather than the internal channels of SWNTs. Filling single-walled nanotubes with iodine could be accomplished only in 2002,[93] however, the conductivity of the intercalated nanotubes was not studied.

Considering the nonequivalence of positions in internal channels of SWNTs and in pores between nanotubes, the reported quantitative estimate of conductivity changes [121] cannot be regarded as unquestionably reliable, although, qualitatively, the existence of a charge transfer effect in intercalated SWNTs could be established. Furthermore, a possibility of directed modification of the transport characteristics of nanotubes by intercalating electron-acceptor compounds was demonstrated.[121]

In 2002, in studying the electrical conductivity of the C_{60}@SWNT composites, it was found [122] that they possess lower conductivity than that of unfilled tubes, which prompted a conclusion that charges are localized on the defects of nanotubes filled with fullerene molecules.

The simulation of nanocrystal structures encapsulated into an SWNT cavity makes a great contribution to the understanding of the properties of '1D-crystal@SWNT' composites.[28] The possibility of a transition of the HgTe nanocrystals from semimetallic to semiconductive state upon their insertion into SWNTs, and also the possibility of effective interaction of a nanocrystal with nanotube walls was demonstrated theoretically.[96] In this work, the effectiveness of the determination of the atomic and electronic structures of '1D-crystal@SWNT' nanocomposites with the aid of experimental research and quantum chemical calculations was shown for the first time.

Theoretical studies published so far are devoted in most cases to the magnetism of nanocomposites [particularly, Cu@SWNT (see Ref. 123) and Fe@SWNT (see Refs 33, 124)].† The results of modelling demonstrate that copper nanoparticles experience strong uniform compression in the nanotube channel, which increases with temperature and reaches 2.5 GPa at 800 °C.[123] For the iron clusters (Fe_5 to Fe_{26}) and nanowires encapsulated in SWNTs, the iron–carbon interaction, where charge transfer from iron to carbon occurs, is observed.[33] With the increase in the SWNT diameters, the interaction of Fe atoms with C atoms gradually weakens, and then completely ceases.

The charge transfer is also reduced and the magnetic moment of an iron nanoparticle approaches that in the bulk metal. A substantial change in the band structure of SWNTs upon encapsulation of the Fe_5, Fe_9 and Fe_{13} clusters was demonstrated.[33] On the whole, the magnetic moment of iron clusters encapsulated in SWNTs is lower than that of free clusters: for Fe_{13} within the SWNT(8,8) it is equal to 2.30 μ_B.[124] For iron nanowires in SWNT channels, an increase in the magnetic moment due to the reduction in the coordination number of iron atoms located on the surface is observed. The thinner the nanowire the larger its magnetic moment.[124]

To date, in the majority of experimental studies on the properties of '1D-crystal@SWNT' systems, data on the chemical and structural changes of intercalated compounds are primarily provided, whereas information on the physical properties of these composites is contained merely in isolated publications (see, for instance, Refs 14, 125, 126), although investigations into the physical properties are essential for the practical application of '1D-crystal@SWNT' composites.

The presence of an electron transfer between intercalated particles and nanotube walls can be determined not only by changes in transporting characteristicts but also by changes in the Raman spectra of '1D-crystal@SWNT' composites.[13, 14, 30, 94, 97] Indeed, recently it has theoretically been proven that intercalation of single-walled nanotubes with electron-donor (or electron-acceptor) compounds results in an effective increase (or decrease) in electron density on the SWNT walls, which increases (or lowers) the Fermi energy (Fig. 19).[127] Doping SWNTs with electrons leads to filling of the SWNT π*-orbitals and, as a consequence, to weakening of the C–C-bonds, which

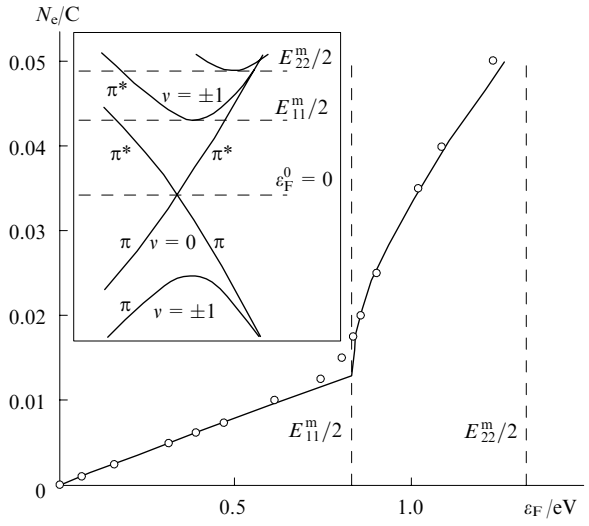


Figure 19. Charge calculation for the SWNT(9,9) (N_e/C is the number of electrons that correspond to one carbon atom) as a function of the Fermi energy (ε_F) of the nanotube at 20 °C.[127]
The insert is calculation of the electronic structure of the SWNT(9,9) near the Kelvin point.

appears as a shift in the radial breathing mode (RBM, the spectrum region $< 200\ cm^{-1}$), which corresponds to the synchronous radial vibrations of carbon atoms (A_{1g}), and in the G-mode (the spectrum region between 1500 and 1600 cm^{-1}) that pertains to the C–C-bond vibrations (E_{2g}) [128, 129] to a low-energy region of the Raman spectra (Fig. 20 *a*,*b*).[31] Conversely, upon intercalation of electron acceptors into SWNTs, a decrease in electron density on the SWNT π*-orbitals is observed, which appear as shifts in the RBM- and G-bands in the Raman spectra to a high-energy region of the spectrum (Fig. 20 *c*,*d*).[13]

A shift in the RBM-mode frequencies of the composites can also be associated with mechanical deformations of nanotubes in a radial direction (with their contraction or expansion) [129, 130] caused by intercalated material. Such spectral changes allow the Raman spectroscopy to be utilized for the qualitative determination of structural deformations of SWNTs and nanocrystals, and also for

† The Cu@SWNT and Fe@SWNT composites have not been obtained so far.

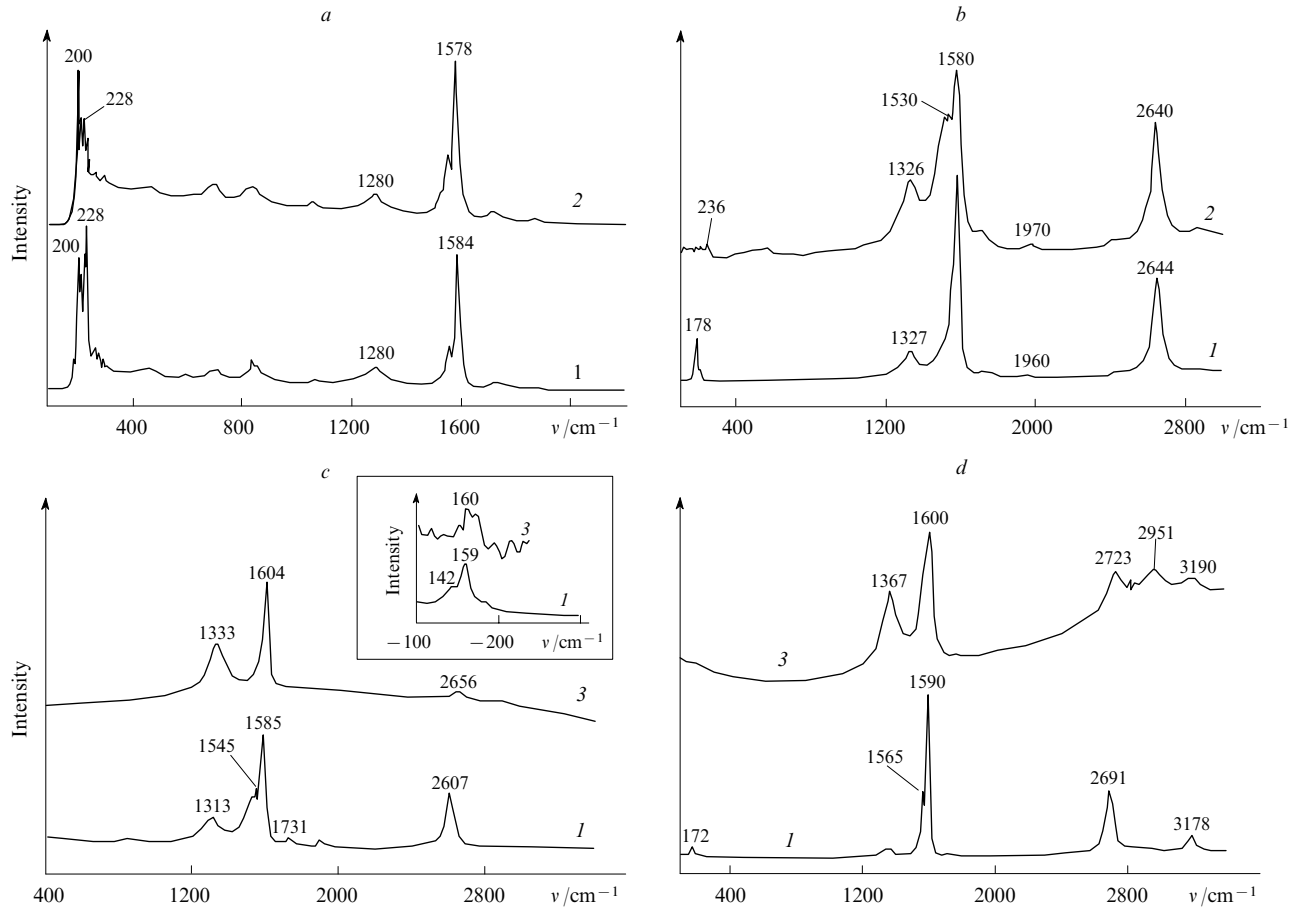


Figure 20. The Raman spectra of pure SWNTs (spectrum *1*), and also the Ag@SWNT (spectrum *2*) and CrO_3@SWNT (spectrum *3*) composites registered at the excitation energies 1.58 eV (782 nm) (*a*), 2.41 eV (514.5 nm) (*b*), 1.96 eV (632.8 nm) (*c*) and 2.71 eV (457.9 nm) (*d*).[13]

the detection of possible chemical interactions between NT walls and an introduced substance.

The filling yield ‡ of SWNTs with inorganic compounds can be determined from the value of a shift in G-bands, which reaches 15–20 cm^{-1} as compared to their positions in unfilled SWNTs, and also from the change in the profile of the G-peak, *i*.e., its width and area.[13, 30, 94, 97, 127]

To date, the vibrational spectra of SWNTs filled with both electron-donor (Ag, Li, Rb, K, Cs), and electron-acceptor compounds (Br_2, I_2, CrO_3, PbO, PbI_2, LiCl, NaCl, KCl, $CaCl_2$) have been studied.[13, 30, 94, 97, 121, 131–138] As already mentioned above, in the Raman spectra of '1D-crystal@SWNT' composites significant shifts in the RBM- and G-bands are observed, which depend on the chemical properties of an encapsulated compound.[13] Thus in the spectra of the Ag@SWNT composite recorded at the excitation energy 1.58 eV, shifts in G-bands to lower frequencies by ~6 cm^{-1} occur (from 1584 cm^{-1} for the SWNT to 1578 cm^{-1} for the Ag@SWNT composite), and the intensities of the RBM-peaks at 200 and 228 cm^{-1} (Fig. 20 *a*) also change. The CrO_3@SWNT system at the excitation energy 1.96 eV exhibits shifts in G-bands to a high-energy region by 19 cm^{-1} (from 1585 cm^{-1} for the SWNT to1604 cm^{-1} for CrO_3@SWNT) (Fig. 20 *c*), and also the disappearance of the RBM-peak at 142 cm^{-1} and a shift in the RBM-band at 159 cm^{-1} (to 160 cm^{-1}, the inset in Fig. 20 *c*), which suggests a loss of resonance for the nanotubes of diameter 1.71 nm (the RBM-mode at 142 cm^{-1}) upon intercalation of an electron acceptor into SWNTs and also testifies to a structural deformation of the SWNT (contraction of the SWNTs upon crystallization of chromium oxide in their channels). These results provide evidence for the effective charge transfer Ag → SWNT and SWNT → CrO_3.

Note that registration of the Raman spectra at different excitation energies makes it possible to obtain a more detailed insight into the eletronic structure of '1D-crystal@SWNT' systems with nanotubes of different chirality, since the resonance conditions are satisfied, depending on the laser energy, only for certain SWNT types.[129, 139–142] Fig. 20 *b*,*d* depicts the Raman spectra of the Ag@SWNT and CrO_3@SWNT composites recorded at the excitation energies 2.41 and 2.71 eV, respectively.[13] Interestingly, in the case of unfilled SWNTs with diameter of 1.0–1.5 nm the excitation of only semiconducting nanotubes takes place at these energies, whereas in the case of composites (especially Ag@SWNT) the excitation of only metallic nanotubes is observed. These results suggest strong carbon — intercalated metal interaction, which can result in not only a shift in the Fermi level, but also in a rearrangement of SWNT band structure caused by charge transfer.[28]

‡ The filling yield is assessed by the number of electrons corresponding to one carbon atom.

Studies on SWNTs intercalated with electron acceptors (S, Se, Te) demonstrated that the values of RBM- and G-mode shifts to higher frequencies evenly increase with the electronegativity of the introduced atoms. This is due to an increase in the effectiveness of electron density transfer from SWNT carbons to the chalcogens.[143] According to the data from the resonance Raman spectroscopy, shifts in RBM- and G-bands in the spectra of the X@SWNT (X = S, Se, Te) composites with various nanotube types substantially differ, which testifies to a selective impact of chalcogen nanoparticles on the electronic structures of SWNTs. This assumption was justified by the data from TEM: an increase in the degree of crystallinity of the encapsulated compounds was observed on going from sulfur to tellurium, which relates to the increase in the covalent radius of a chalcogen and to the adjustment of a one-dimensional nanocrystal structure to the diameter of an SWNT.

A comprehensive examination of MHal@SWNT (M = K, Cu, Ag; Hal = Cl, Br, I) nanocomposites by the Raman spectroscopy showed that the electron density transfer between intercalated crystals of MHal and and nanotube walls is governed not only by the electron affinity of the Hal anion, but also by the structure of a crystal as well as by the character of the M–Hal bond.[105,144] Thus in the KI@SWNT composites the electronic interaction between KI crystals and SWNT carbon atoms is absent, whereas in the CuHal@SWNT and AgHal@SWNT composites a strong interaction of copper and silver halides, which are electron acceptors, with the SWNT carbon atoms is observed. This results in a considerable change in the electronic structures of the nanotubes, *viz*., a descrease in the Fermi level resulting in a shift of G-bands to higher frequencies by 18–23 cm^{-1}. It was established that the values of these shifts depend on the chemical nature of nanoparticles to be encapsulated into SWNTs and increase with the increase in the electron affinities of halogens in the I → Br → Cl series, which allowed one to suppose a mechanism of charge transfer from nanotube walls to intercalated nanocrystals through halogen atoms.

Electronic interaction between SWNTs and the CuHal and AgHal one-dimensional crystals was more pronounced in the case of metallic nanotubes, which was also confirmed by the data from optical absorption spectroscopy of the CuI@SWNT and AgI@SWNT nanocomposites. The conclusion about charge transfer from the SWNT walls to the halogen atoms was also confirmed by X-ray photoelectron spectroscopy (XPS). In the XPS spectra of the nanocomposites, a shift of the C_{1s} band to lower energies (by ~0.4 eV) was observed, which suggests the emergence of a positive charge on the nanotube carbon atoms. However, a quantitative assessment of the charge on the C atoms is complicated owing to a change in photoelectric work function upon the intercalation of a substance into the nanotube. The descrease in electron density on walls of metallic nanotubes in the MHal@SWNT (M = Cu, Ag; Hal = Cl, Br, I) nanocomposites leads to transition of the metallic nanotubes to a semiconductive state,[105,145,146] while electron beam-induced deintercalation of a part of material incorporated into NT channels[110] enables a controlled p–n-junction in a single SWNT.

In examining the Raman spectra of charged SWNTs (the charging of the SWNTs was carried out in an electrochemical cell with platinum electrodes modified with the purified SWNTs; a 0.2 M solution of $LiClO_4$ in acetonitrile was used as the electrolyte) it was found that shifts of the G^+- and G^--components of the G-mode to higher frequences occur irrespective of the applied potential (Fig. 21).[147] This fact suggests an ambiguity in the interpretation of the electron density displacement in '1D-crystal@SWNT' nanocomposites by shifts of phonon vibrations in the Raman spectra. The application of the given method to the exploration of the charged AgI@SWNT nanocomposites (charging was carried out in an electrochemical cell with platinum electrodes modified with the AgI@SWNT nanocomposite, a 0.2 M solution of $LiClO_4$ in 1,2-dimethoxyethane was used as the electrolyte) enabled an exact determination of the direction and value of a transferred charge in '1D-crystal@SWNT' nanocomposites by shifts of the G^+- and G^--components (Fig. 22).[146] Thus, despite the complexity of a direct determination of the direction of charge transfer in '1D-crystal@SWNT' nanocomposites by Raman spectroscopy data, combined spectral and electrochemical studies at different potentials permit the shift of the Fermi energy upon the intercalation of various compounds to be established.

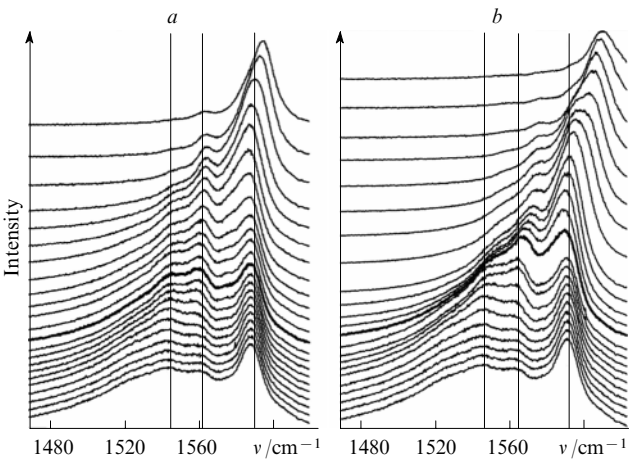


Figure 21. The Raman spectra of charged SWNTs at the excitation energy 1.92 eV.[147]
The nanotubes were charged by applying the potential difference 0 to −1.5 V (*a*) and from 0 to 1.5 V (*b*). In the area 0 to 0.7 V (or −0.7 V) potential was changed with an interval of 0.05 V, while in the region 0.7 V (or −0.7 V) to the maximum potential 1.5 V (or −1.5 V), with an interval of 0.1 V (the spectra are presented bottom to top).

It should be noted that D-lines in the Raman spectra that appear in the region 1300–1350 cm^{-1} for nanotubes are also sufficiently informative. Their analysis allows one to obtain a qualitative picture of changes in the structures of single-walled nanotubes upon their filling. In a number of studies, an increase in the intensity of the D-peak in the '1D-crystal@SWNT' composites as compared to that in pure nanotubes has been revealed (see Fig. 20 *b*–*d*), which is associated with a decrease in the degree of order of SWNTs upon their filling with nanoparticles.[13,136]

Transformations of the electronic structure of pure nanotubes upon their filling can be evaluated not only by changes in the Raman spectra, but also by alterations in electronic absorption spectra. Thus changes in intensities of the major absorption bands (up to their complete disappearance) of semiconducting (E_{11}^{s}, E_{22}^{s}) and metallic (E_{11}^{m}) SWNTs upon their p- and n-doping (for instance, with Li atoms, Fig. 23) are reported.[135] In addition, in the Raman

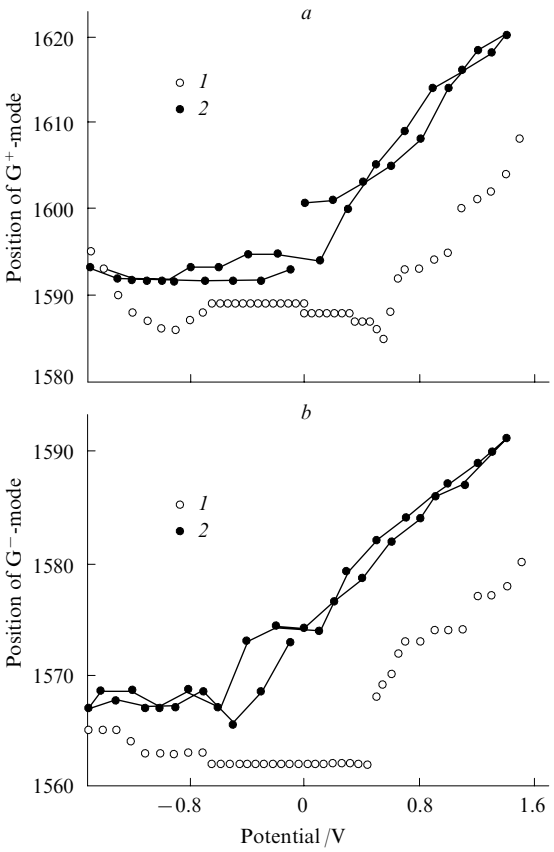


Figure 22. The positions of the maxima of the G^+- and G^--components in the Raman spectra of a pure SWNT (*1*) and the AgI@SWNT (*2*) nanocomposite (excitation energy is 1.92 eV) obtained by *in situ* charging of nanotubes by applying the potential difference in the range −1.5 to 1.5 V.[146]

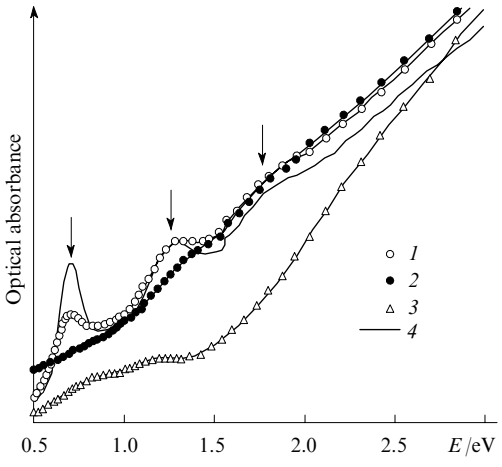


Figure 23. Evolution of the optical absorption spectra of the Li_xC@SWNT composites with different stoichiometries.[135] $x = 0.04$ (*1*), 0.14 (*2*), 0.17 (*3*). For comparison, an absorption spectrum of pure SWNTs is provided (*4*).

spectra of the composites, an increase in the background signal, band shifts by 0.1–0.2 eV (for example, for $Li_{0.17}C$ in Fig. 23) and the appearance of new absorption bands can be observed.[135] The majority of the observed changes can be explained on the basis of a charge transfer mechanism within the model of a rigid band structure. Upon n-doping of SWNTs, electrons fill the conduction band, whereas on p-doping, electrons are removed from that band, which can lead to the prohibition of some optical transitions (in many respects, this applies to the transitions between the first van Hove singularities — E_{11}^{s} and E_{11}^{m}). Thus gradual removal of electrons from the populated states of SWNTs results in quenching of the E_{11}^{s}-transitions.

VI. Conclusion

The intercalation of inorganic compounds into single-walled nanotubes allows directed alteration of the electronic properties of SWNTs. Thus the encapsulation of electron acceptors (MHal, where M = Cu, Ag; Hal = Cl, Br, I) into metallic nanotubes results in an electron density transfer from SWNT walls to the one-dimensional crystal, which gives rise to a transition of the system to a semiconducting state. Conversely, the encapsulation of electron donors into the channels of semiconductive SWNTs can lead to the emergence of electronic conductivity of a '1D-crystal@SWNT' composite, resulting from an increase in electron density on the nanotube walls. Such an approach makes it possible to control the electronic structures of SWNTs as well as to develop ground-breaking nanosystems such as quantum threads,[120] single nanotubes with a p–n-transition, and nanocables (in the case of the intercalation of a conductor into a semiconducting nanotube).[148] In this connection, nanocomposites based on single-walled nanotubes are regarded as extremely promising for application as elements of nanoelectronics.

One of recent studies [149] demonstrated the possibility of creating efficient elecrodes for symmetric supercondensers based on the CrO_3@SWNT composites that allow exceptionally high charging rates to be achieved owing to reactions between the CrO_x nanocrystals and the electrolyte. Tubes filled with the CuI nanocrystals are characterized by a low photoelectric work function, which can be exploited in manufacturing field effect emitters for modern electroluminescent tubes and X-ray minitubes.[150] These are just first examples of the utilization of unique properties of intercalated SWNTs, the real scope of applicability of such nanocomposites defies assessement as yet. Further development of the techniques of intercalation of various compounds into internal channels of SWNTs as well as of the analytical methods for studying such nanocomposites is required.

We expect that the data presented in this review will encourage the development of new approaches to the preparation, research and application of low-dimensional nanostructures based on carbon nanotubes.

The authors express their thanks to the research group of the Laboratory of Electron Microscopy, A V Shubnikov Institute of Crystallography of the RAS, for fruitful discussions and for providing research results. This work was carried out within the framework of the Federal Targeted Scientific and Technological Programme (Project No. 02.513.12.3012).

References

1. S Iijima, T Ichihashi *Nature (London)* **363** 603 (1993)
2. D S Bethune, C H Klang, M S de Vries, G Gorman, R Savoy, J Vazquez, R Beyers *Nature (London)* **363** 605 (1993)
3. S Iijima *Nature (London)* **354** 56 (1991)

4. R Saito, R Saito, M Fujita, M Fujita, G Dresselhaus, G Dresselhaus, M S Dresselhaus, M S Dresselhaus *Appl. Phys. Lett*. **60** 2204 (1992)
5. M S Dresselhaus, G Dresselhaus, R Saito *Carbon* **33** 883 (1995)
6. S J Tans, A R M Verschueren, C Dekker *Nature (London)* **393** 49 (1998)
7. J C Charlier, P Lambin *Phys. Rev. B* **57** R15037 (1998)
8. J W G Wilder, L C Venema, A G Rinzler, R E Smalley, C Dekker *Nature (London)* **391** 59 (1998)
9. T W Odom, J L Huang, P Kim, C M Lieber *Nature (London)* **391** 62 (1998)
10. T W Odom, J L Huang, P Kim, C M Lieber *J. Phys. Chem. B* **104** 2794 (2000)
11. P X Hou, C Liu, H M Cheng *Carbon* **46** 2003 (2008)
12. P Chaturvedi, P Verma, A Singh, P K Chaudhary, Harsh, P K Basu *Defence Sci. J*. **58** 591 (2008)
13. P Corio, A P Santos, P S Santos, M L A Temperini, V W Brar, M A Pimenta, M S Dresselhaus *Chem. Phys. Lett*. **383** 475 (2004)
14. M Monthioux, E Flahaut, J P Cleuziou *J. Mater. Res*. **21** 2774 (2006)
15. M S Arnold, A A Green, J F Hulvat, S I Stupp, M C Hersam *Nat. Nanotechnol*. **1** 60 (2006)
16. R Saito, G Dresselhaus, M S Dresselhaus *Phys. Rev. B* **53** 2044 (1996)
17. J C Charlier, T W Ebbesen, P Lambin *Phys. Rev. B* **53** 11108 (1996)
18. M Ouyang, J L Huang, C M Lieber *Acc. Chem. Res*. **35** 1018 (2002)
19. J U Lee, P P Gipp, C M Heller *Appl. Phys. Lett*. **85** 145 (2004)
20. H J Dai, J Kong, C W Zhou, N Franklin, T Tombler, A Cassell, S S Fan, M Chapline *J. Phys. Chem. B* **103** 11246 (1999)
21. P C Collins, M S Arnold, P Avouris *Science* **292** 706 (2001)
22. V Derycke, R Martel, J Appenzeller, P Avouris *Nano Lett*. **1** 453 (2001)
23. A Bachtold, P Hadley, T Nakanishi, C Dekker *Science* **294** 1317 (2001)
24. A Bachtold, P Hadley, T Nakanishi, C Dekker *Physica E* **16** 42 (2003)
25. G Brown, S R Bailey, M Novotny, R Carter, E Flahaut, K S Coleman, J L Hutchison, M L H Green, J Sloan *Appl. Phys. A: Mater. Sci. Process*. **76** 457 (2003)
26. G Brown, S R Bailey, J Sloan, C G Xu, S Friedrichs, E Flahaut, K S Coleman, J L Hutchison, R E Dunin-Borkowski, M L H Green *Chem. Commun*. 845 (2001)
27. J L Hutchison, N Grobert, R M Zakalyukin, A A Eliseev, M V Chernisheva, A S Kumnskov, Y V Grigoriev, A V Krestinin, B Freitag, N A Kiselev *AIP Conf. Proc*. **999** 79 (2008)
28. P N D'yachkov *Uglerodnye Nanotrubki: Stroenie, Svoistva, Primeneniya* (Carbon Nanotubes. Structure, Properties and Applications) (Moscow: Binom, 2006)
29. E L Sceats, J C Green, S Reich *Phys. Rev. B* **73** 125441 (2006)
30. S B Fagan, A G S Filho, J M Filho, P Corio, M S Dresselhaus *Chem. Phys. Lett*. **406** 54 (2005)
31. H Kataura, Y Maniwa, M Abe, A Fujiwara, T Kodama, K Kikuchi, H Imahori, Y Misaki, S Suzuki, Y Achiba *Appl. Phys. A: Mater. Sci. Process*. **74** 349 (2002)
32. M M Rahman, M Kisaku, T Kishi, T A Roman, W A Dino, H Nakanishi, H Kasai *J. Phys. Soc. Jpn*. **74** 742 (2005)
33. M Weissmann, G Garcia, M Kiwi, R Ramirez, C C Fu *Phys. Rev. B* **73** 125435 (2006)
34. J Sloan, A I Kirkland, J L Hutchison, M L H Green *Chem. Commun*. 1319 (2002)
35. M Monthioux *Carbon* **40** 1809 (2002)
36. J Sloan, A I Kirkland, J L Hutchison, M L H Green *C. R. Phys*. **4** 1063 (2003)
37. Y K Chen, A Chu, J Cook, M L H Green, P J F Harris, R Heesom, M Humphries, J Sloan, S C Tsang, J F C Turner *J. Mater. Chem*. **7** 545 (1997)
38. Z X Zhang, Z Y Pan, Q Wei, Z J Li, L K Zang, Y X Wang *Int. J. Mod. Phys. B* **17** 4667 (2003)
39. M L Cohen *AIP Conf. Proc*. **590** 297 (2001)
40. M H Du, H P Cheng *Phys. Rev. B* **68** 113402 (2003)
41. S Okada *Phys. Rev. B* **72** 153409 (2005)
42. Y F Li, T Kaneko, T Ogawa, M Takahashi, R Hatakeyama *Chem. Commun*. 254 (2007)
43. P M Ajayan, S Iijima *Nature (London)* **361** 333 (1993)
44. M R Pederson, J Q Broughton *Phys. Rev. Lett*. **69** 2689 (1992)
45. M Monthioux, E Flahaut *Mater. Sci. Eng. C* **27** 1096(2007)
46. J Sloan, R E Dunin-Borkowski, J L Hutchison, K S Coleman, V C Williams, J B Claridge, A P E York, C Xu, S R Bailey, G Brown, S Friedrichs, M L H Green *Chem. Phys. Lett*. **316** 191 (2000)
47. E G Rakov, in *Nanomaterials Handbook* (Ed. Y Gogotsi) (London: CRC Press, 2006)
48. S Seraphin, D Zhou, J Jiao, J C Withers, R Loutfy *Nature (London)* **362** 503 (1993)
49. A Leonhardt, A Ritschel, R Kozhuharova, A Graff, T Muhl, R Huhle, I Monch, D Elefant, C M Schneider *Diam. Relat. Mater*. **12** 790 (2003)
50. J Y Dai, J M Lauerhaas, A A Setlur, R P H Chang *Chem. Phys. Lett*. **258** 547 (1996)
51. C-H Kiang, J-S Choi, T T Tran, A D Bacher *J. Phys. Chem. B* **103** 7449 (1999)
52. F Beguin, E Flahaut, A Linares-Solano, J Pinson *Lect. Notes Phys*. **667** 495 (2006)
53. P M Ajayan, T W Ebbesen *Rep. Prog. Phys*. **60** 1025 (1997)
54. N Demoncy, O Stephan, N Brun, C Colliex, A Loiseau, H Pascard *Eur. Phys. J., B* **4** 147 (1998)
55. A Loiseau, H Pascard *Chem. Phys. Lett*. **256** 246 (1996)
56. M Monthioux, B W Smith, B Burteaux, A Claye, J E Fischer, D E Luzzi *Carbon* **39** 1251 (2001)
57. J Liu, A G Rinzler, H J Dai, J H Hafner, R K Bradley, P J Boul, A Lu, T Iverson, K Shelimov, C B Huffman, F Rodriguez-Macias, Y S Shon, T R Lee, D T Colbert, R E Smalley *Science* **280** 1253 (1998)
58. S C Tsang, Y K Chen, P J F Harris, M L H Green *Nature (London)* **372** 159 (1994)
59. B C Satishkumar, A Govindaraj, J Mofokeng, G N Subbanna, C N R Rao *J. Phys. B: At. Mol. Opt. Phys*. **29** 4925 (1996)
60. B W Smith, D E Luzzi *Chem. Phys. Lett*. **321** 169 (2000)
61. H Z Geng, X B Zhang, S H Mao, A Kleinhammes, Y Wu, O Zhou *Abstr. Pap. Am. Chem. Soc*. **229** U919 (2005)
62. J Chancolon, F Archaimbault, A Pineau, S Bonnamy *J. Nanosci. Nanotechnol*. **6** 82 (2006)
63. C Pan, M S Chandrasekharaiah, D Agan, R H Hauge, J L Margrave *J. Phys. Chem*. **96** 6752 (2002)
64. K Hirahara, K Suenaga, S Bandow, H Kato, T Okazaki, H Shinohara, S Iijima *Phys. Rev. Lett*. **85** 5384 (2000)
65. T Okazaki, T Shimada, K Suenaga, Y Ohno, T Mizutani, J Lee, Y Kuk, H Shinohara *Appl. Phys. A: Mater. Sci. Process*. **76** 475 (2003)
66. A V Eletskii *Usp. Fiz. Nauk* **174** 1191 (2004) [*Physics-Uspekhi* **47** 1119 (2004)]
67. A L Ivanovskii *Zh. Neorg. Khim*. **48** 1 (2003) [a]
68. P M F J Costa, J Sloan, T Rutherford, M L H Green *Chem. Mater*. **17** 6579 (2005)
69. J Sloan, D M Wright, H G Woo, S Bailey, G Brown, A P E York, K S Coleman, J L Hutchison, M L H Green *Chem. Commun*. 699 (1999)
70. A A Eliseev, M V Chernysheva, N I Verbitskii, E A Kiseleva, A V Lukashin, Y D Tretyakov, N A Kiselev, O M Zhigalina, R M Zakalyukin, A L Vasiliev, A V Krestinin, J L Hutchison, B Freitag *Chem. Mater*. **21** 5001 (2009)
71. E Dujardin, T W Ebbesen, H Hiura, K Tanigaki *Science* **265** 1850 (1994)
72. T W Ebbesen *J. Phys. Chem. Solids* **57** 951 (1996)
73. E Dujardin, T W Ebbesen, A Krishnan, M M J Treacy *Adv. Mater*. **10** 1472 (1998)
74. D Ugarte, A Chatelain, W A deHeer *Science* **274** 1897 (1996)
75. D Ugarte, T Stockli, J M Bonard, A Chatelain, W A de Heer *Appl. Phys. A: Mater. Sci. Process*. **67** 101 (1998)
76. G Korneva, Y G Gogotsi, D Halverson, G Friedman, J-C Bradley, K G Kornev *Nano Lett*. **5** 879 (2005)

77. A Hashimoto, H Yorimitsu, K Ajima, K Suenaga, H Isobe, A Miyawaki, M Yudasaka, S Iijima, E Nakamura *Proc. Natl. Acad. Sci. USA* **101** 8527 (2004)
78. J Sloan, J Hammer, M Zwiefka-Sibley, M L H Green *Chem. Commun.* 347 (1998)
79. A V Eletskii *Usp. Fiz. Nauk* **167** 945 (1997) [*Physics-Uspekhi* **40** 899 (1997)]
80. J Mittal, M Monthioux, H Allouche, O Stephan *Chem. Phys. Lett.* **339** 311 (2001)
81. X R Ye, Y H Lin, C M Wang, M H Engelhard, Y Wang, C M Wai *J. Mater. Chem.* **14** 908 (2004)
82. Z Y Sun, L Fu, Z M Liu, B X Han, Y Q Liu, J M Du *J. Nanosci. Nanotechnol.* **6** 691 (2006)
83. E H Lock, W Merchan-Merchan, J D'Arcy, A V Saveliev, L A Kennedy *J. Phys. Chem. C* **111** 13655 (2007)
84. Z M Liu, B X Han *Adv. Mater.* **21** 825 (2009)
85. J Xie, X B Zhao, G S Cao, M J Zhao *Electrochim. Acta* **50** 2725 (2005)
86. L Q Jiang, L Gao *Chem. Mater.* **15** 2848 (2003)
87. A N Khlobystov, D A Britz, J W Wang, S A O'Neil, M Poliakoff, G A D Briggs *J. Mater. Chem.* **14** 2852 (2004)
88. C G Xu, J Sloan, G Brown, S Bailey, V C Williams, S Friedrichs, K S Coleman, E Flahaut, J L Hutchison, R E Dunin-Borkowski, M L H Green *Chem. Commun.* 2427 (2000)
89. P M Ajayan, O Stephan, P Redlich, C Colliex *Nature (London)* **375** 564 (1995)
90. S Friedrichs, U Falke, M L H Green *ChemPhysChem.* **6** 300 (2005)
91. J Sloan, S Friedrichs, R R Meyer, A I Kirkland, J L Hutchison, M L H Green *Inorg. Chim. Acta* **330** 1 (2002)
92. A I Kirkland, M R Meyer, J Sloan, J L Hutchison *Microsc. Microanal.* **11** 401 (2005)
93. X Fan, E C Dickey, P C Eklund, K A Williams, L Grigorian, R Buczko, S T Pantelides, S J Pennycook *Phys. Rev. Lett.* **84** 4621 (2000)
94. M Hulman, M Hulman, H Kuzmany, H Kuzmany, M F J Costa Pedro, P M F J Costa, S Friedrichs, S Friedrichs, L H Green Malcolm, M L H Green *Appl. Phys. Lett.* **85** 2068 (2004)
95. N Thamavaranukup, H A Hoppe, L Ruiz-Gonzalez, P M F J Costa, J Sloan, A Kirkland, M L H Green *Chem. Commun.* 1686 (2004)
96. R Carter, J Sloan, A I Kirkland, R R Meyer, P J D Lindan, G Lin, M L H Green, A Vlandas, J L Hutchison, J Harding *Phys. Rev. Lett.* **96** 215501 (2006)
97. E Flahaut, J Sloan, S Friedrichs, A I Kirkland, K S Coleman, V C Williams, N Hanson, J L Hutchison, M L H Green *Chem. Mater.* **18** 2059 (2006)
98. J Sloan, M C Novotny, S R Bailey, G Brown, C Xu, V C Williams, S Friedrichs, E Flahaut, R L Callender, A P E York, K S Coleman, M L H Green, R E Dunin-Borkowski, J L Hutchison *Chem. Phys. Lett.* **329** 61 (2000)
99. H Shiozawa, T Pichler, C Kramberger, A Gruneis, M Knupfer, B Buchner, V Zolyomi, J Koltai, J Kurti, D Batchelor, H Kataura *Phys. Rev. B* **77** 153402 (2008)
100. C Kramberger, H Rauf, M Knupfer, H Shiozawa, D Batchelor, A Rubio, H Kataura, T Pichler *Phys. Rev. B* **79** 195442 (2009)
101. H Shiozawa, T Pichler, C Kramberger, M Rummeli, D Batchelor, Z Liu, K Suenaga, H Kataura, S R P Silva *Phys. Rev. Lett.* **102** 046804 (2009)
102. J Cao, J L Sun, J Hong, H Y Li, H Z Chen, M Wang *Adv. Mater.* **16** 84 (2004)
103. M Nath, P V Teredesai, D V S Muthu, A K Sood, C N R Rao *Curr. Sci. India* **85** 956 (2003)
104. Y Q Liu, L Gao *Mater. Chem. Phys.* **91** 365 (2005)
105. M V Chernysheva, Candidate Thesis in Chemical Sciences, Moscow State University, Moscow 2008
106. R Pfeiffer, H Kuzmany, T Pichler, H Kataura, Y Achiba, M Melle-Franco, F Zerbetto *Phys. Rev. B* **69** 035404 (2004)
107. R Meyer, J Sloan, R E Dunin-Borkowski, A I Kirkland, M C Novotny, S R Bailey, J L Hutchison, M L H Green *Science* **289** 1324 (2009)
108. B W Smith, M Monthioux, D E Luzzi *Nature (London)* **396** 323 (1998)
109. A N Khlobystov, D A Britz, A Ardavan, G A D Briggs *Phys. Rev. Lett.* **92** 245507 (2004)
110. N A Kiselev, R M Zakalyukin, O M Zhigalina, N Grobert, A S Kumskov, Y V Grigoriev, M V Chernysheva, A A Eliseev, A V Krestinin, Y D Tretyakov, B Freitag, J L Hutchison *J. Microsc.* **232** 335 (2008)
111. J S Bendall, A Ilie, M E Welland, J Sloan, M L H Green *J. Phys. Chem. B* **110** 6569 (2006)
112. S Friedrichs, R R Meyer, J Sloan, A I Kirkland, J L Hutchison, M L H Green *Phys. Solid State* **44** 463 (2002)
113. R R Meyer, J Sloan, R E Dunin-Borkowski, A I Kirkland, M C Novotny, S R Bailey, J L Hutchison, M L H Green *Science* **289** 1324 (2000)
114. A K Ivanov-Shitz *Crystallogr. Rep.* **52** 302 (2007)
115. J Krug, L Sieg *Phys. Chem.* **7** 739 (1952)
116. N A Kiselev, R M Zakalyukin, A S Kumskov, A L Vasil'ev, A V Krestinin, M V Chernysheva, A A Eliseev *2-ya Shkola 'Metrologiya i Standartizatsiya v Nanotekhnologiyakh i Nano-industrii. Prostranstvennye Kharakteristiki Nanomaterialov i Nanostruktur' (Tez. dokl.), Chernogolovka, 2009* [The 2nd School 'Metrology and Standardization in Nanotechnologies and Nanoindustry. Spatial Characteristics of Nanomaterials and Nanostructures (Abstracts of Reports), Chernogolovka, 2009]
117. R N Schock, J C Jamieson *J. Phys. Chem. Solids* **30** 1527 (1969)
118. P W Bridgman *Proc. Am. Acad. Arts Sci.* **76** 1 (1945)
119. J Sloan, S J Grosvenor, S Friedrichs, A I Kirkland, J L Hutchison, M L H Green *Angew. Chem., Int. Ed.* **41** 1156 (2002)
120. J J Zhao, R H Xie *J. Nanosci. Nanotechnol.* **3** 459 (2003)
121. L Grigorian, K A Williams, S Fang, G U Sumanasekera, A L Loper, E C Dickey, S J Pennycook, P C Eklund *Phys. Rev. Lett.* **80** 5560 (1998)
122. H Hongo, F Nihey, M Yudasaka, T Ichihashi, S Iijima *Physica B* **323** 244 (2002)
123. Y Guo, Y Kong, W Guo, H Gao *J. Comput. Theor. Nanosci.* **1** 93 (2004)
124. Y J Kang, J Choi, C Y Moon, K J Chang *Phys. Rev. B* **71** 115441 (2005)
125. V V Khvostov, L A Chernozatonskii, Z Ya Kosakovskaya, V V Babaev, M B Guseva *Pis'ma Zh. Eksp. Teor. Fiz.* **56** 280 (1992) [b]
126. E G Gal'pern, A R Sabirov, I V Stankevich, A L Chistyakov, L A Chernozatonskii *Fiz. Tv. Tela* **44** 599 (2002) [c]
127. N Caudal, A M Saitta, M Lazzeri, F Mauri *Phys. Rev. B* **75** 115423 (2007)
128. A M Rao, E Richter, S Bandow, B Chase, P C Eklund, K A Williams, S Fang, K R Subbaswamy, M Menon, A Thess, R E Smalley, G Dresselhaus, M S Dresselhaus *Science* **275** 187 (1997)
129. M S Dresselhaus, G Dresselhaus, A Jorio, A G Souza, R Saito *Carbon* **40** 2043 (2002)
130. A Jorio, M A Pimenta, A G Souza, R Saito, G Dresselhaus, M S Dresselhaus *New J. Phys.* **5** 157 (2003)
131. A M Rao, P C Eklund, S Bandow, A Thess, R E Smalley *Nature (London)* **388** 257 (1997)
132. S Gupta, M Hughes, A H Windle, J Robertson *J. Appl. Phys.* **95** 2038 (2004)
133. N Bendiab, E Anglaret, J L Bantignies, A Zahab, J L Sauvajol, P Petit, C Mathis, S Lefrant *Phys. Rev. B* **64** 245424 (2002)
134. N Bendiab, A Righi, E Anglaret, J L Sauvajol, L Duclaux, F Beguin *Chem. Phys. Lett.* **339** 305 (2001)
135. J L Sauvajol, N Bendiab, E Anglaret, P Petit *C. R. Phys.* **4** 1035 (2003)
136. P Puech, A Bassil, J Gonzalez, C Power, E Flahaut, S Barrau, P Demont, C Lacabanne, E Perez, W S Bacsa *Phys. Rev. B* **72** 155436 (2005)
137. M Sendova, E Flahaut, B DeBono *J. Appl. Phys.* **98** (2005)

138. K R Kissell, K B Hartman, P A W Van der Heide, L J Wilson *J. Phys. Chem. B* **110** 17425 (2006)
139. A Jorio, C Fantini, M A Pimenta, R B Capaz, G G Samsonidze, G Dresselhaus, M S Dresselhaus, J Jiang, N Kobayashi, A Gruneis, R Saito *Phys. Rev. B* **71** 075401 (2005)
140. M S Dresselhaus, P C Eklund *Adv. Phys.* **49** 705 (2000)
141. S D M Brown, P Corio, A Marucci, M S Dresselhaus, M A Pimenta, K Kneipp *Phys. Rev. B* **61** R5137 (2000)
142. M S Dresselhaus, G Dresselhaus, in *Carbon Nanotubes* (Ed. Ph Avouris) (Berlin, Heidelberg: Springer, 2001)
143. M V Chernysheva, E A Kiseleva, N I Verbitskii, A A Eliseev, A V Lukashin, Y D Tretyakov, S V Savilov, N A Kiselev, O M Zhigalina, A S Kumskov, A V Krestinin, J L Hutchison *Physica E* **40** 2283 (2008)
144. M V Kharlamova, M M Brzhezinskaya, A S Vinogradov, I P Suzdalev, Yu V Maksimov, V K Ishmennik, S V Novichikhin, A V Krestinin, L V Yashina, A V Lukashin, Yu D Tretyakov, A A Eliseev *Ros. Nanotekhnol.* **4** 77 (2009) [d]
145. M V Chernysheva, A A Eliseev, A V Lukashin, Y D Tretyakov, S V Savilov, N A Kiselev, O M Zhigalina, A S Kumskov, A V Krestinin, J L Hutchison *Physica E* **37** 62 (2007)
146. A A Eliseev, L V Yashina, M V Kharlamova, N I Verbitsky, M V Chernysheva, M Brzhezinskaya, A S Vinogradov, A V Krestinin, N A Kiselev *Carbon* **47** (2009) (in the press)
147. M Kalbac, L Kavan, L Dunsch, M S Dresselhaus *Nano Lett.* **8** 1257 (2008)
148. Z Zhou, J J Zhao, Z F Chen, X P Gao, J P Lu, P V Schleyer, C K Yang *J. Phys. Chem. B* **110** 2529 (2006)
149. G Lota, E Frackowiak, J Mittal, M Monthioux *Chem. Phys. Lett.* **434** 73 (2007)
150. A A Zhukov, A A Eliseev, M V Chernysheva, V K Gartman, D N Borisenko *Pis'ma Zh. Eksp. Teor. Fiz.* **90** (2009) [b] (in the preess)

[a] — *Russ. J. Inorg. Chem. (Engl. Transl.)*
[b] — *J. Exp. Theor. Phys. Lett. (Engl. Transl.)*
[c] — *Phys. Solid State (Engl. Transl.)*
[d] — *Nanotechnol. Russ. (Engl. Transl.)*